CHAPTER 8

CONCLUSIONS

8.1 BEAMING FRACTION

From the results of chapter 7 we come to the important conclusion that pulsar beams are not one-sided. We now calculate the beaming fraction f for each pulsar in our pruned sample under the following assumptions:

(1) The angle α between the rotation axis $\vec{\Omega}$ and the magnetic axis $\vec{\mu}$ is randomly distributed between 0° and 90° (so that the probability of obtaining α is proportional to $\sin\alpha$). Actually the results of chapter 7 seem to suggest that small values of α are preferred. We arrived at a similar conclusion in one of our recent exercises in which we fit the <u>observed</u> distribution of duty-cycles ($= W_{e/p} \times 360^\circ$), in a given period range, to the distribution expected on the basis of radom orientation of the line of sight and the magnetic axis with respect to the rotation axis. From this exercise we conclude that α may not be larger than $\sim 75^\circ$. However, we do not consider these evidences as conclusive. Therefore we allow α to take on all possible angles. It must be noted that in our geometry $0^\circ \leq \alpha \leq 90^\circ$; i.e., we do not discriminate between the case when $\vec{\Omega}.\vec{\mu} < 0$ and the case when $\vec{\Omega}.\vec{\mu} > 0$. It is

quite natural to expect qualitative differences in pulsar electrodynamics in the two cases; however, it is not clear that the pulsar beam geometry shoud be different in the two cases.

(2) The angle $\alpha + \beta$ between rotation axis and the line of sight is distributed randomly. We allow β to take on all values between $-\beta_{max}$ and $+\beta_{max}$, where $2\beta_{max}$ is the North-South dimension of the pulsar beam. If pulsar beams were indeed one-sided as claimed by Arons (1979) and co-workers, then $-\beta_{max} \leq \beta \leq 0$. This would affect the beaming fraction by a factor of 2, which is quite significant.

(3) The mean East-West dimension of pulsar beams is $\sim 17^{\circ}$ of longitude. To obtain this we have to first compute the mean <u>observed</u> East-West dimension $\langle W_{10} \rangle_{obs}$ (corresponding to pulse width W_{10}). In this calculation we need to prune pulsars on the basis of two criteria. Firstly, some high dispersion measure pulsars would exhibit artificially large pulse widths due to inter stellar scattering. Secondly, some W_{10} quoted in the catalogue of Manchester and Taylor (1981) include the width of the interpulse also (e.g., the Crab pulsar), thus inflating the actual W_{10}. Therefore in the above calculation we excluded those pulsars whose duty-cycles were larger than 50°. We obtain the mean $\langle W_{10} \rangle_{obs}$ for the remaining pulsars to be 20.9°. From this we obtain the actual east-west dimension by firstly reducing it by $2/\pi$ due to the averaging over α and $\alpha+\beta$; in addition, if the pulsar beam cross-sectin is an ellipse, $\langle W_{10} \rangle_{obs}$ has to be further enhanced by $4/\pi$ to account for the averaging over the ellipse. We thus obtain

$$\langle W_{10} \rangle_{actual} = \langle W_{10} \rangle_{obs} \times \frac{2}{\pi} \times \frac{4}{\pi} = 17^{\circ} \qquad (8.1)$$

Actually, the pulse width data suggests that W_{10} decreases weakly with increasing period. However, this variation is small and so we have ignored this aspect here.

(4) the beam elongation varies according to eq. (6.14).

Now the beaming fraction f is defined as the raio of the effective solid angle Ω_{PSR} in which a pulsar is visible to the total solid angle 4π. For a beam of North-South dimension 2θ radians, Ω_{PSR} is obtained by averaging the solid angle corresponding to 2θ over all allowed values of α and $\alpha+\beta$. We obtain

$$\Omega_{PSR} = \pi \sin\theta \left[2\pi - 4\theta\right] + 4\pi \left[1 - \cos\theta\right] \qquad (8.2)$$

Figure 8.1 shows the variation of f implied by eq. (6.14) and eq. (8.2). The beaming fraction is ~ 1.0 at small periods and decreases asymptotically to ~ 0.2 at large periods. For a mean beam elongation R of ~ 3.0, f is ~ 0.5, assuming again that the mean East-West dimension is $\sim 15^{\circ}$. Note that in this caculation the East-West dimension is relevant only insofar as it determines the North-South dimension. We recall that Kundt (1977, 1981) had for long been suggesting that pulsar beams may be elongated, and that the beaming fraction f may be closer to 1.0 than to 0.2.

8.2 BIRTHRATE

We have computed the current $\overline{J}_{P,est}$ (defined in eq. (4.7)) by means of the following formula

$$\overline{J}_{P,est}(P_{min}, P_{max}) = \frac{1}{P_{max} - P_{min}} \sum_{i=1}^{N} \frac{1}{f(P_i)} S(L_i, P_i)\, \dot{P}_i, \quad P_{min} \leq P \leq P_{max} \qquad (8.3)$$

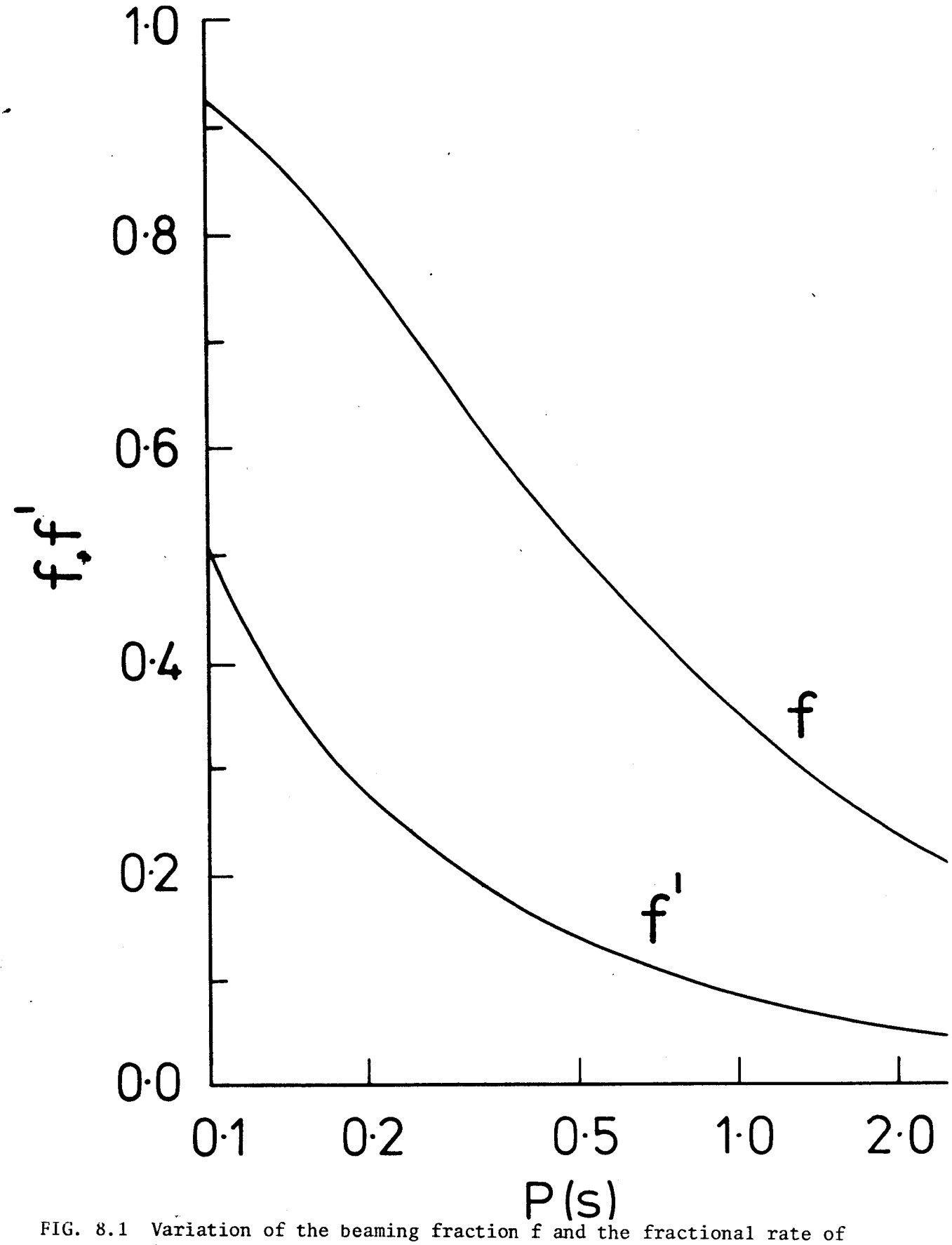

FIG. 8.1 Variation of the beaming fraction f and the fractional rate of interpulse occurrence f' with pulsar period, corresponding to the variation of R shown in Figure 6.3. f is evaluated as $\langle\Omega_{PSR}\rangle/4\Pi$, where $\langle\Omega_{PSR}\rangle$ is the total solid angle over which the rotating pulsar is visible, suitably averaged over all values of α. f' is similarly $\langle\Omega_I\rangle/\langle\Omega_{PSR}\rangle$, where $\langle\Omega_I\rangle$ is the solid angle over which interpulses are visible (including both single and double pole interpulses).

It differs from eq. (4.7) in that each pulsar is now given a specific beaming fraction $f(P_i)$ which depends upon the period. The currents in the three period bins (as in fig. 4.2) are shown in fig. 8.2. As before we compute the birthrate from the plateau value of J_p .

$$b = \bar{J}_{p,est}(0.4502, 0.8268) = 0.035^{+0.035}_{-0.020} \text{ PSRs yr}^{-1} \text{ G}^{-1} \qquad (8.4)$$

or one pulsar born every 28^{+40}_{-14} years in the Galaxy. This value represents a decrease by a factor of ~ 2 over the conventionally quoted birthrates (Manchester and Taylor 1977; Lyne 1981). This is due to the incresed beaming fraction whose average value now is ~ 0.5 instead of ~ 0.2. In eq. (8.4) we used the scale values $S(L_i, P_i)$ instead of $S'(P_i, \dot{P}_i)$ so that our calculation is model-independent. It now becomes interesting to compare our estimated pulsar birthrate with the supernova rate. A reliable estimate of the supernova rate is unfortunately not available. It is obtained both from direct observations of supernova explosions in external galaxies and from a study of historical supernovae as well as the supernova remnants in our galaxy. Estimates from studies of external galaxies range right from one explosion every 359 years (Zwicky 1962) to one every 11 years (Tamman 1977). Studies of historical supernovae in our galaxy have yielded one explosion every 30 years (Katgert and Oort 1967; Clark and Stephenson 1977). Studies of supernova remnents in our galaxy have given one explosion every 60 years (Poveda and Woltjer 1968; Milne 1970; Downes 1971). However, two recent works (Higden and Lingenfelter 1980; Srinivasan and Dwarakanath 1982) on supernova remnants have estimated that the explosions in the galaxy occur once every 25 to 30 years. If we accept this number, there is no significant discrepancy between

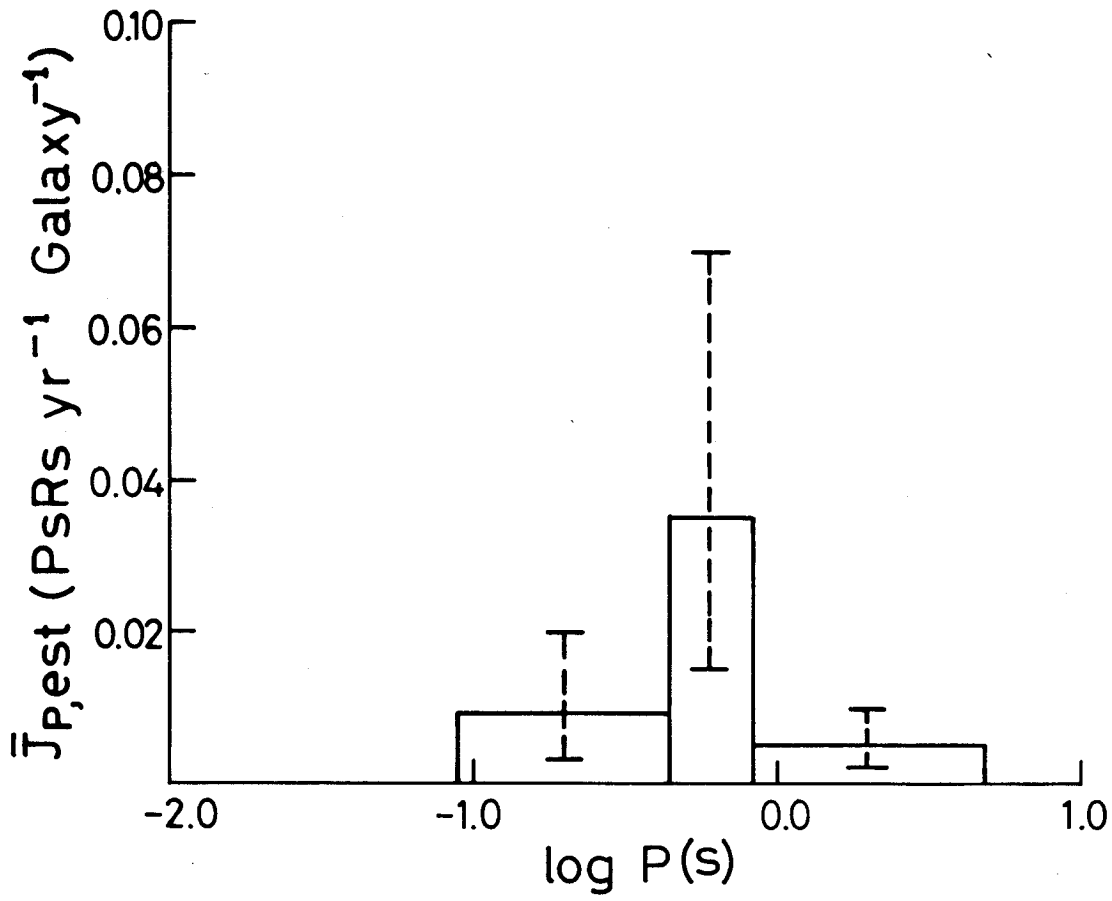

FIG. 8.2 : Current $J_{p,est}$ (estimated by eq. (8.3)) in equal number bins in period. Each bin contains $\sim$ 55 pulsars. The error bars represent the 95% confidence limits, whose computation is explained in Appendix C. Scale values S(L,P) have been used.

the birthrate of pulsars and the occurence rate of supernovae.

8.3 INJECTION

We see from fig. 8.2 that the current in bin 2 continues to be higher than the current in bin 1. There is a significant increase in the level of injection over that shown by fig. 4.2. This is because pulsars in the first bin are now more observable than pulsars in the second bin, on account of the evolving radio beams. From fig. 8.2 we conclude that the percentage of injected pulsars is now definitely more than 30% (maybe almost 50%). In section 5.4 we offered two possible explanations for injection. We find the latter explanation (that neutron stars switch on as radio pulsars only after they are $\sim 10^5$ years old) appealing, for it helps to resolve the observed lack of association between pulsars and supernova remnants (this has already been discussed in section 5.4).

8.4 IMPLICATIONS OF THE ANALYSIS

In sections 8.1 to 8.3 we summarised the basic results of this thesis. If our results are taken seriously, then there are several important implications for pulsars in general.

In chapter 2 we derived the scale height z_0 of thermal electrons to be very large (~1000 pc). Our tests reject low values of z_0 . This might have some relevence to the applicability of the McKee and Ostriker (1977) model for the interstellar medium (ISM) where the ionized component (HII) of

the ISM is mostly associated with the neutral hydrogen (HI) clouds. Since HI clouds have a scale height of ~ 170 pc (Crovisier 1978), the same value is implied for the HII and hence n_e . Our test, however, shows that this is unlikely.

In chapter 6 we showed that the large discrepancy, between the observed distribution of the polarisation angle swings 2θ (and the angle gradient $|d\theta/d\varphi|^{-1}_{max}$) and the currently accepted version of the RC model coupled with circular beams, can be reconciled if we assume that pulsar beams are highly elongated. Now, pulsar beams are believed to be hollow cones (Komesaroff 1970) because of the frequent occurence of double and muliple component pulse profiles. Tables 6.3a to 6.3c give the pulse types of many of the pulsars as identified by Manchester and Taylor (1977, tables 2 and 3), using the morphological classification scheme of Taylor and Huguenin (1971). The single component profiles (type S) are commonly considered to be outer cuts of the beam while the doubles and multiples (type C, for complex) are believed to be inner cuts intersecting the hollow part. The maximum values of $|\frac{d\theta}{d\varphi}|^{-1}_{max}$ among the type C pulsars in table 6.3a to 6.3c are 0.103, 0.103 and 0.100, respectively. These values are remarkably equal suggesting that the North-South dimension of the central hollow region does not evolve with P . Taking α_{eff} to be 60°, eq. (6.20) shows that the inner North- South diameter of the hollow cone is $\sim 10^\circ$. Further, from Manchester and Taylor (1977, table 22) we find that the mean component separation in 22 type C pulsars to be $\sim 10.8^\circ$. Again taking α_{eff} to be 60° and allowing for averaging over an elliptic beam (requiring factors of $\sin(60^\circ)$ and $\pi/2$) we estimate the

East-West peak-to-peak distance to be $\sim 15^{\circ}$; the corresponding diameter of the hollow region should hence be $\sim 10^{\circ}$. we thus reach the interesting conclusion that the central hollow region of the pulsar beam is essentially circular and apparently does not evolve with the pulsar period. This result is independent of α_{eff} since the esimates of both the North-South and East-West dimensions scale essentially as $\sin \alpha_{eff}$ Figure 8.3 summarizes the picture of pulsar beams that emerges from our results. Note that at short periods the beam is extremely large, extending $\sim 100^{\circ}$ in latitude.

One of the hitherto unsolved problems in pulsars is the occurence of interpulses in only short period pulsars. For instance among the thirty pulsars in table 6.3a-c, interpulses are observed in 3 pulsars, viz., PSR 0950+08, PSR 1929+10 and PSR 0531+21, in the short period group, in 2 pulsars viz.,PSR 0823+26 and PSR 1944+17 (Hankins 1980), in the medium period group (but both have fairly short period, $<$ 0.6 s.), and in none of the long period pulsars. The evolution of the beam elongation could be a natural explanation for this observation. Figure 8.1 shows the estimate of the fractional rate of occurence of interpulses f' as a function of period. We have assumed that R has the variation shown in eq. (6.14), that α is uniformly disttributed on a sphere, and that interpulses can occur either from the opposite pole to the main pulse or the same pole. From fig. 8.1 we estimate that 3.1 ± 1.2 out of the 10 pulsars in table 6.3a should have interpulses, the corresponding numbers for tables 6.3b and 6.3c being 1.3 ± 1.1 and 0.6 ± 0.8, respectively. While the good quantitative agreement with the actual numbers observed may be fortuitous, we

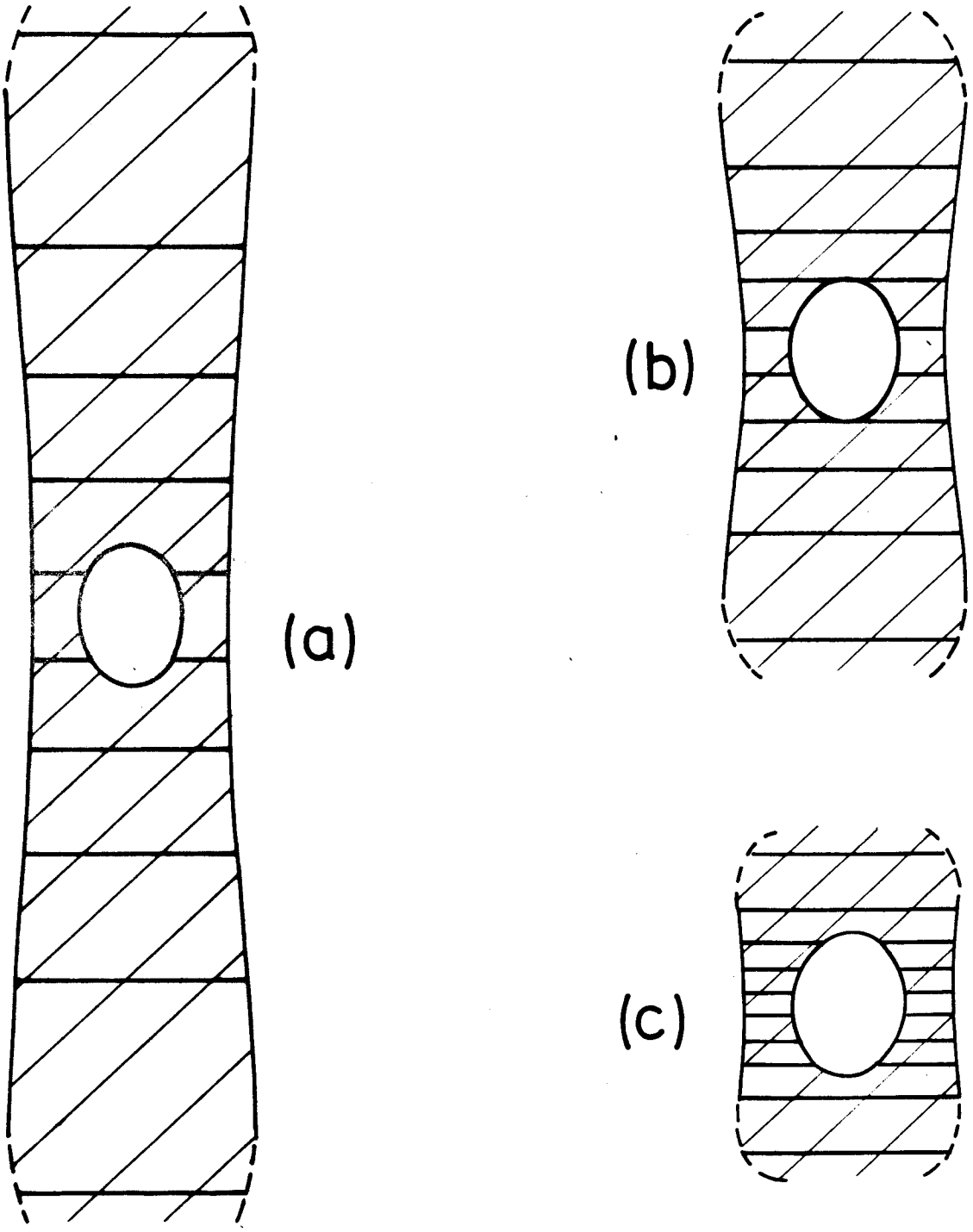

FIG. 8.3 Mean pulsar beams, drawn to scale, corresponding to the period ranges (a) $P < 0.388s$, (b) $0.388s < P < 1.2s$ and (c) $1.2s < P$. Radio radiation is received from the hatched regions. The horizontal lines are ieadlized lines of sight spaced at 10% probability intervals and have been calculated assuming a gaussian variation of probability. The outer extremities of the beams have been represented by dashed lines since the beams may not have a firm boundary but probably fade away gradually. The dumb-bell beam shape is suggested by the statistics of pulse width data. While the beam elongation reduces dramatically with increasing period, the hollow region in the centre seems to be essentially period-independent. If complex pulse profiles are identified with lines of sight which intersect the central hollow, then only 1 or 2 pulsars out of 10 in (a) are expected to have such profiles while in (b) and (c) we expect $\sim$3 and $\sim$6 out of 10 respectively.

believe our explanation is qualitatively correct.

Another interesting observation in pulsars is that type C profiles occur predominantly in long period pulsars. Vivekanand and Radhakrishnan (1980) suggested that pulse inensity could be modulated across the polar cap due to evolving irregularities in eiher the surface relief or the local magnetic field. Our results give an alternate explanation. We find that the outer North-South dimension of the beam has a strongly variable elongation while the dimension of the inner hollow region is essentially independent of P . Thus only a small fraction of small period pulsars (typically 1 or 2 out of 10) will intersect the central hollow region to produce a complex profile, while we typically expect about 3 type C pulsars out of 10 in the medium P pulsars, and more than half the long period pulsars should be type C. These numbers are generally in agreement with the actual observations (table 6.3, where we take pulsars labelled S? to be type C).

Our results might also be compatible with the occurence of drifing sbpulses in only long P pulsars. If this phenomenon is caused by circular motion of the emission zone around the magnetic pole (Ruderman and Sutherland 1975), then it is reasonable that it would occur in a nearly circular beam like fig. 8.3c but it would be rather difficult to envisage in elongated beams such as in figs. 8.3a or 8.3b.

The variation of $\dot{f}$ with P could be important for statistical studies of pulsar evolution. An important requirement for these studies is that one should identify a

range of P and a range of $\dot{P}$ (since one normally employs the P-$\dot{P}$ diagram) where there is no birth or death of pulsars. Our results show that pulsars are dying at all values of P due to beam shrinkage. Until this effect can be properly quantified eq. (6.14) should be considered only as an initial estimate and requires careful refinement with more data), all results on pulsar evolution such as the estimate of the braking index, the decay time of the magnetic field, etc., should be treated with caution.

An interesting point worth noting is that beam shrinkage is a new mechanism for pulsar death, which has not been considered so far. Some of the scenarios considered usually for pulsar death include decay of the magnetic field (Flowers and Ruderman 1977) and alignment of the magnetic dipole moment with the rotation axis (Jones 1976). Lyne et al. (1975) have pointed out that a line of the form $\dot{P}P^{-5} = \text{const.}\ (\sim 5\times10^{-17})$ seems to describe an empirical cut-off for pulsar activity, and they explained it as representing a constant field stength at the light-cylinder. Ruderman and Sutherland (1975) considered the variation of the accelerating potential acting on the charged particles in their model and predicted a line of the form $\dot{P}^2P^{-5} = \text{const.}$ We offer yet another explanation here. The number of pulsars within observable range of a survey is proportional to the luminosity (assuming a two dimensional spatial distribution) which varies as $P^{-0.9}\dot{P}^{0.5}$ (see chapter 5). Combined with the variation of the beaming fraction $f \propto R \propto P^{-0.65}$, this gives an overall variation of the form $P^{-1.55}\dot{P}^{0.5}$. This suggests that pulsar death or rather thinning out, should be described by lines of constant $\dot{P}P^{-3}$. Of course in this case one does not expect the

apparently abrupt cut-off that is observed.

To our knowledge none of the current pulsar theories predicts the high elongation of pulsar beams, its evolution with period and apparent lack of correlation with any other pulsar parameter. A reanalysis of the theories keeping these clues in mind appears worthwhile.

Mon. Not. R. astr. Soc. (1983) **204**, *Short Communication*, 81P–85P

Improved parameters for 40 pulsars

M. Vivekanand *Raman Research Institute, Bangalore 560080, India*
D. K. Mohanty and C. J. Salter *Tata Institute of Fundamental Research Centre, Indian Institute of Science Campus, PO Box 1234, Bangalore 560012, India*

Received 1983 May 24

Summary. Improved declinations have been measured for 40 weak pulsars with the Ooty Radio Telescope, together with flux densities at 327 MHz. For 32 of the pulsars, improved periods have been derived. It is demonstrated that PSR1922 + 20 is highly unlikely to be associated with the radio continuum source 4C 20.48.

1 Introduction

The recent pulsar catalogue of Manchester & Taylor (1981), referred to below as MT, contains a number of objects whose declinations are uncertain to at least a few arcmin. The present work was undertaken to measure improved declinations for many of these objects with the Ooty radio telescope.

The pulsars observed were selected from the MT compilation using three criteria:

(i) the declinations had published uncertainties of $\geqslant 5$ arcmin;
(ii) the sources lay within the declination range of the Ooty radio telescope, $|\delta| \leqslant 35°$;
(iii) the time-averaged flux densities at 400 MHz were $\geqslant 5$ mJy.

To the 38 pulsars resulting from this selection were added two with flux densities somewhat below this limit. One, PSR1926 +18, lies near the HC40 emission complex (Velusamy & Kundu 1974), lending it intrinsic interest. For the other, PSR1922 + 20, Mantovani *et al.* (1982) have shown that the continuum radio source 4C 20.48 lies within the published errors of the pulsar position. It was hoped that a more accurate declination for this pulsar would throw light on the possibility of an association between the two objects.

2 Observations and analysis

The observations were made between 1983 January 25 and March 23. The Ooty radio telescope was used in the total-power mode in conjunction with the 144-channel pulsar receiver. In this mode each of the 12 telescope beams has a half-power beamwidth of $2° \times 5.5 \sec \delta$

arcmin, the individual beams being separated in declination by 3 sec δ arcmin. The 144-channel receiver permits the recording of 12 frequency-channels (bandwidth ≈ 300 kHz) for each beam, giving an effective total bandwidth of about 4 MHz. For each beam, data from the individual frequency channels are combined off-line with the appropriate time delays to 'de-disperse' the observed pulsar. The receiver time-constant was about 20 ms and the data were sampled at intervals of 16 ms. The data for each beam were folded with the predicted pulsar topocentric period to yield a pulse profile for each beam. Following detection of a pulsar the north–south beamshape of the telescope was fitted to the observed response of the source in adjacent beams, giving the nominal declination of the source.

The observing time spent on each pulsar was chosen to provide an expected signal-to-noise ratio of > 10. This resulted in integration times between 16 and 80 min. For practical reasons, data from only the central eight telescope beams were recorded. If a pulsar was not detected within the comb of beams centred on the declination catalogued by MT, further observations were taken 12 arcmin to the north and south. This declination coverage proved sufficient for detection of all the objects in our observing list. A number of the pulsars were measured independently on two or more occasions to check the internal consistency of the results. Additionally, on each day we observed a pulsar whose declination was known to better than 5 arcsec in order to check the absolute consistency of the observations.

A careful calibration of the telescope pointing as a function of declination was made at the beginning of the experiment using strong continuum radio sources. This was checked in detail on a number of occasions during the experiment and found to have the same form. At least one continuum source was observed each day to determine the absolute offset of the pointing curve.

The flux density scale of the observations was set by measurements of the radio source 3C 161, assumed to have a flux density of 48 Jy at 327 MHz, consistent with the flux density scale of Baars *et al.* (1977). In deriving the mean observed flux densities of the pulsars, corrections for the background continuum radiation were made using brightness temperatures estimated from the 408-MHz all-sky survey of Haslam *et al.* (1982) and adopting a temperature spectral index of 2.6 between 327 and 408 MHz.

3 Results

The final declinations and mean flux densities derived for the 40 pulsars are given in Table 1, together with the flux densities of the pulsars of known declination that were observed daily. When more than one measurement of a source was made, the average value is given.

Where a pulsar was detected with a reasonable signal-to-noise ratio in three adjacent beams, a standard error in the measured declination of ± 30 arcsec is expected. For an object detected in only two adjacent beams, the equivalent error is ± 45 arcsec. One pulsar, PSR 1740–03, was detected at only the 4.5 σ level and an error of ± 60 arcsec is applicable. The daily observations of pulsars of accurately known position were reduced in the same way as those of the 40 sample sources. Almost all were detected in three adjacent beams and the mean declination difference, defined as (actual – measured) was – 15 ± 7 arcsec, with the standard deviation on a single measurement being 24 arcsec. It is thus possible that a small systematic error of about one-twentieth of the telescope half-power beamwidth exists in the measured declinations. For sample pulsars observed on two or more occasions, the internal consistency of the declination measurements is in good accord with our quoted uncertainties.

Our derived mean flux densities were compared with those given in MT for 408 MHz. For sources of flux density $S > 10$ mJy at both 327 and 408 MHz, the mean flux density ratio $S(237)/S(408)$ is 1.4 ± 0.1, with the standard deviation on an individual ratio being 0.55.

Table 1. Pulsar declinations, periods and flux densities.

PSR	Dec (1950.0) (° ′ ″)	± (″)	Period (ns)	Overall error (ns)	Epoch JD−2440000	Flux density (mJy)
0559 − 05	–	–	–	–	–	15
0656 + 14	14 18 31	45	384 863 839	6	4327.50	11
0740 − 28	–	–	–	–	–	227
0853 − 33	− 33 19 58	45	1 267 532 672	22	4328.50	18
0940 + 16	16 45 08	45	1 087 417 727	23	4329.00	15
1010 − 23	− 23 23 02	30	2 517 944 579	33	4328.01	8
1039 − 19	− 19 26 07	30	1 386 367 735	19	4329.01	10
1552 − 31	− 31 25 07	30	518 109 751.4	4	4328.01	23
1552 − 23	− 23 33 10	30	532 577 402	4	4328.03	3
1600 − 27	− 27 04 12	30	778 311 740	6	4328.04	19
1604 − 00	–	–	–	–	–	38
1612 − 29	− 29 32 38	45	2 477 567 322	19	4327.00	7
1620 − 09*	− 09 01 13	45	1 276 444 847	13	4328.00	5
1632 + 24	24 39 56	45	–	–	–	9
1649 − 23	− 23 58 40	45	–	–	–	9
1700 − 32	− 32 51 22	30	1 211 784 624	14	2005.1	55
1700 − 18	− 18 41 28	30	–	–	–	16
1702 − 19*	− 19 01 34	30	298 985 852.1	1.5	4326.98	30
1717 − 29	− 29 30 09	45	620 447 861	7	2005.0	41
1718 − 32	− 32 05 04	30	477 157 077.4	5	2005.1	74
1730 − 22	− 22 26 43	45	871 682 810	11	2005.0	29
1732 − 07	− 07 22 57	30	–	–	–	38
1738 − 08	–	–	–	–	–	11
1740 − 03	− 03 36 08	60	444 644 291	14	4328.99	2.5
1742 − 30	− 30 39 02	30	367 421 492.9	4	2005.1	105
1745 − 12	–	–	–	–	–	36
1754 − 24	− 24 21 40	30	234 094 343	12	4327.98	50
1756 − 22	− 22 05 33	30	460 969 062.1	1.4	4327.98	36
1804 − 27	− 27 15 40	30	827 770 612	3	4326.98	23
1813 − 26	− 26 50 55	30	592 885 093	7	2004.6	24
1819 − 22	− 22 57 58	45	1 874 267 731	20	2004.7	31
1820 − 31	− 31 08 16	30	284 052 887.6	0.7	4326.98	42
1821 − 19	–	–	–	–	–	44
1826 − 17	− 17 52 45	45	307 129 196.8	3	2005.1	86
1831 − 03	− 03 40 55	30	686 676 816	8	2004.3	107
1834 − 10	–	–	–	–	–	50
1846 − 06	− 06 40 26	30	1 451 292 579	16	2005.2	49
1859 + 03	–	–	–	–	–	276
1900 + 06	06 11 25	30	–	–	–	28
1900 + 01	–	–	–	–	–	78
1900 − 06	− 06 36 30	45	431 884 718.9	4	2004.8	63
1920 + 20	20 12 16	45	–	–	–	4
1920 + 21	–	–	–	–	–	40
1922 + 20	20 34 06	30	237 790 138	8	3957.99	4
1926 + 18	18 39 50	30	–	–	–	3
1929 + 20	–	–	–	–	–	57
1937 − 26	− 26 08 54	45	402 857 434.1	1.5	4326.98	12
1942 − 00	− 00 48 14	45	1 045 630 957	10	4329.01	8
1943 − 29	− 29 21 02	30	959 447 364	5	4326.98	10
1946 − 25	− 25 32 17	45	957 615 458	5	3956.54	4
2110 + 27	27 43 21	30	–	–	–	24
2113 + 14	–	–	–	–	–	8

* Pulsar designation is changed by the improved declination measurement.

This mean value implies a spectral index of about 1.6 between the two frequencies, consistent with that expected from previous work (i.e. McLean 1973). The standard deviation on a single ratio of about 40 per cent of the mean value is considered to be satisfactory in view of the contributory factors. Apart from the intrinsic experimental errors on the 327- and 408-MHz measurements, and the residual effects of interstellar scintillation, pulsars themselves are highly variable. Additionally, the Ooty radio telescope accepts only a single linearly polarized component of the incident radiation. Thus, for a significantly linearly polarized pulsar, our measurements will contain an additional uncertainty which could be particularly marked for objects of lower rotation measure (an object of rotation measure $150\,\mathrm{rad\,m^{-2}}$ will have a 180° rotation of its plane of polarization across the 4-MHz bandwidth).

With a time constant of some 20 ms most of the observed pulsars showed unresolved, or only marginally resolved, integrated pulse profiles, although we find broadened trailing edges to the profiles of a number of pulsars of higher dispersion measure. This is believed to be due to interstellar scattering and will be discussed in another paper.

4 Discussion

Lyne, Ritchings & Smith (1975) and Ashworth & Lyne (1981) have published accurate period measurements made at Jodrell Bank for a large number of weak pulsars. The overall error of their period determinations were set by uncertainties in the positions of the pulsars rather than by the measurements themselves. We have used our improved declination determinations, together with the right ascensions from MT, to re-evaluate these periods and reduce the overall errors. This re-evaluation was made for 32 pulsars using an ephemeris generated at theLincoln Laboratory, MIT. The updated periods and their overall errors are given in Table 1, together with the appropriate epoch. The overall errors in the table include positional terms and the statistical errors published by the Jodrell Bank workers and represent the formal standard deviation.

The improved declination measurement for PSR1922 + 20 seems to resolve the possibility that the object is coincident with the continuum source 4C 20.48. The revised position for the pulsar lies well outside the confines of the continuum source, even allowing for the error given in Table 1. In fact, the pulsar is separated from the centre of 4C 20.48 by some 10 σ. This is compatible with the conclusion of Mantovani *et al.* (1982) that the continuum source has an extragalactic origin.

Acknowledgments

We thank T. Velusamy for bringing the positional proximity of PSR1926 + 18 and HC40 to our notice. S. Krishna Mohan kindly provided the data reduction program used in this experiment. The satisfactory completion of this experiment was made possible only by the skill and assistance of the Ooty radio telescope observers, T. L. N. Babu Mallerji, B. Jaison, P. K. Manoharan, K. Ramesh and V. Venkatsubramani. R. Balasubramanian maintained the 144-channel receiver over the period of observation. Miss N. N. Shanthakumari is thanked for typing the manuscript.

References

Ashworth, M. & Lyne, A. G., 1981. *Mon. Not. R. astr. Soc.*, **195**, 517.
Baars, J. W. M., Genzel, R., Pauliny-Toth, I. I. K. & Witzel, A., 1977. *Astr. Astrophys.*, **61**, 99.
Haslam, C. G. T., Salter, C. J., Stoffel, H. & Wilson, W. E., 1982. *Astr. Astrophys. Suppl.*, **47**, 1.

Lyne, A. G., Ritchings, R. T. & Smith, F. G., 1975. *Mon. Not. R. astr. Soc.*, **171**, 579.
McLean, A. I. O., 1973. *Mon. Not. R. astr. Soc.*, **165**, 133.
Manchester, R. N. & Taylor, J. H., 1981. *Astr. J.*, **86**, 1953.
Mantovani, F., Nanni, M., Salter, C. J. & Tomasi, P., 1982. *J. Astr. Astrophys.*, **3**, 335.
Velusamy, T. & Kundu, M. R., 1974. *Astr. Astrophys.*, **32**, 375.

J. Astrophys. Astr. (1980) 1, 119–128

The Structure of Integrated Pulse Profiles

M. Vivekanand and V. Radhakrishnan *Raman Research Institute, Bangalore 560080*

Received 1980 July 8; accepted 1980 October 9

Abstract. We offer two possible explanations to account for the characteristics of integrated pulse profiles, in particular their degree of complexity, their variation from pulsar to pulsar, their stability, and the tendency of complex profiles to be associated with older pulsars.

It is proposed that the pulse structure could be a reflection of surface irregularities at the polar caps, and it is shown how the surface relief can affect the number of positrons released into the magnetosphere which are subsequently responsible for the observed radio radiation. The electrons produced in the vacuum break-down in the gap carry enough energy to allow creating such a surface relief in $\sim 10^6$ years, and one way in which this could be achieved is discussed.

Alternatively, the presence of multipole components in the magnetic fields of older pulsars could lead to significant variations in the curvature of the field lines across the gap, and hence to structure in the integrated pulse profiles. An assessment of the two hypotheses from observed pulse profiles seems to favour the polar cap relief picture.

Key words : pulsars—integrated pulse profiles—polar cap model

1. Introduction

One of the many remarkable features of pulsar radio radiation is the integrated pulse shape. Barring mode changes which we shall not discuss here it has been well established that the integrated pulse profiles are reproducible at any time; in other words they are stable for periods of time long compared with those over which pulsars have been observed so far. Further it has been noted (Taylor and Huguenin 1971) that in general pulsars with periods less than 0·75 seconds have simple pulse profiles while those with longer periods tend to have complex pulse profiles. This correlation clearly suggests that the pulse profile becomes more complex as the pulsar ages, but no satisfactory explanation has hitherto been advanced either for the existence of such structure or its evolution with pulsar age. This is in contrast to the

microstructure of pulses, drifting sub-pulses, and other short period phenomena for which a number of possible explanations have been advanced.

The observed stability of the integrated pulse structure requires that the information determining its details be stored somewhere on the pulsar. In this paper we investigate two possible ways in which this information could be stored: (a) as surface irregularities at the magnetic polar cap of the pulsar, and (b) as magnetic field variations over the polar cap. We also discuss how this information can become more complex with increasing pulsar age to account for the observed correlation referred to above. We will restrict our discussion to the framework of the RS model (Ruderman and Sutherland 1975) for pulsars and its subsequent modifications (*e.g.* Cheng and Ruderman 1980).

In the model we put forward in this paper, surface irregularities are created by the effect of sparks on local regions in the polar cap. Such irregularities build up over a long period of time and in turn affect the strength of sparks over different areas and the intensity of the associated radio radiation. The minimum scale length of irregularities created by sparks will clearly depend on the area of individual sparks. As a consequence, the maximum number of features so created within the polar cap will depend on the ratio of the polar cap area to that of a spark. The typical area of an individual spark thus plays an important role in the model, and we therefore begin in the next section by estimating it from observations of the pulse microstructure. This is followed by a discussion of the effect of height variations on spark development and the number of positrons released into the magnetosphere by sparks.

In Section 4 we argue that under the combined influence of the temporary heating under a spark and the tension in the surface layer dueto the charge on it, the surface is likely to be deformed by a small amount. It is shown that the deformation required per spark is very small and that enough energy is available to achieve such deformations.

In Section 5 we consider an alternative explanation for the pulse structure based on the presence of multipole components in the magnetic field which are expected to make their appearance with the decay of the pulsar dipole magnetic field (Flowers and Ruderman 1977). In the last section we discuss the relative merits of the two mechanisms and conclude that the presence of several components in the integrated pulse profile of some pulsars favours the polar cap relief model.

2. Microstructure and spark areas

In the RS model the current from the polar cap is interrupted due to the non-availability of positive charges (Fe^{56} ions) which are not pulled off the surface by the electric field generated by the rotation of the neutron star. This causes a vacuum gap to form above the polar cap, about 10^4 cm in both height G and radius L, in which electron-positron pairs are created by any gamma ray photons which happen to be there. These pairs in turn produce photons by curvature radiation which produce more pairs.

This process goes on until the vacuum gap is broken by an avalanche of particles which is called a ' spark '. The positrons travel away from the star to produce the radiation that we see while the electrons go to the polar cap to complete the pulsar

homopolar circuit. The gap is now re-formed and breaks down again by the same process. Such sparks occur about 10^5 times per second providing positron bursts which give rise to the pulsar microstructure, and whose average characteristics are reflected in the integrated pulse profile. We shall now attempt to derive the mean area of a spark from the observations of pulsar microstructure.

Let the area of each spark be a cm^2, and let A cm^2 be the area of the polar cap. Then there are A/a independent sparking regions on the polar cap. If sparks occur at 10 μs intervals, then each area is revisited by a spark after every $A/a \times 10$ μs on the average. Thus an observer would record radiation from sparks at a given location only every $A/a \times 10\mu$s $(= \tau_1)$. The radiation would last for a time τ_2, which we shall discuss later. If sparks occur randomly on the polar cap, the rate of observed sparking would remain the same whether the observer is stationary at a particular longitude on the polar cap or moving across it.

If $\tau_2 < \tau_1$, radiation due to individual sparks can be resolved in each individual pulse of the pulsar, provided the observations are made with fine enough time resolution. If $\tau_2 > \tau_1$, we would only observe a continuous distribution of radiation. If $\tau_2 \approx \tau_1$, we would just resolve individual sparks, but we would interpret $\tau_2 (= \tau_1)$ as a single time scale of intensity variation. All three effects are observed in PSR 0950+08 (Hankins 1971) in which micropulses are spaced from a few hundred μs to 1 ms apart. Their duration ranges from a few hundred μs to as low as 10μs.

We associate the quasi-periodicities of $\lesssim 1$ ms in PSR 1133+16 (Ferguson *et al.* 1976) and in PSR 0950+08 (Hankins 1971) and PSR 2016+28 (Cordes 1976) with the time separation τ_1 of observed sparks. For these pulsars the number of independent sparks area A/a can therefore be estimated to be of the order of $(\tau_1/10\ \mu\text{s}) \lesssim (1\ \text{ms}/10\ \mu\text{s}) = 100$. We thus conclude from the microstructure observations of pulsars that typically there are ten to hundred independent sparking areas on the polar cap. A similar conclusion was reached by Cheng and Ruderman (1977) who found from the widths of drifting subpulses that the fractional area of the polar cap occupied by a spark lies between 10^{-1} and 10^{-2}. We shall take the area of each spark to be $\approx \pi \times 10^8$ cm^2 and the radius of a spark area, assumed circular, to be $R \approx 10^4$ cm.

In passing, a few remarks might be appropriate on the duration τ_2 of the observed microstructure (a few hundred microseconds) which is large compared to the supposed duration of sparks ($\approx 10\mu$s). In the RS model bunches of relativistic particles emit curvature radiation at a particular frequency from a certain extent of the magnetosphere which we will call the radiating zone for that frequency. Thus bunches travelling through the two extremities of this radiating zone would give out radiation which would reach the observer with a spread in time τ_2 which depends upon its extent. Thus τ_2 will depend on the net excess distance travelled by particles to and radiation from one extremity of the radiation zone, over that corresponding to the other.

3. Variations in the polar cap relief

We consider first the possibility that the surface of the polar cap deviates from that of a smooth sphere. It can be shown that the maximum height H of a conical hill on a base of the same material cannot exceed $3\pi Y / \rho g$ where Y is the yield stress.

The value of H depends therefore on Y, ρ, and g all of which have uncertainties associated with them. The value of the Young's modulus for pulsar crustal material was estimated by Irvine (1978) as 10^{19} dynes cm^{-2} based on the value given by Chen, Ruderman and Sutherland (1974) for the binding energy. In view of the later work of Flowers *et al.* (1977) which indicates a decrease in the binding energy, a similar estimate would give a lower value.

If we assume that the yield stress Y is given by the Young's modulus, and lies in the range 10^{18} to 10^{19} dynes cm^{-2}, this leads to a value of H somewhere in the range 1 to 10 cm. We shall assume for the present purpose that H can have a value as high as 10 cm, and discuss later whether and how such irregularities are likely to result from the sparking process. For the moment we shall merely assume that the mean height of a spark area can differ from area to area by as much as 10 cm. The polar gap can then be likened to a parallel plate capacitor of separation G cm whose lower surface has bumps of height H cm and radius l cm. As $G \gg l \gg H$ the fractional excess electric field over the bumps would be $(\Delta\Phi/\Phi) \simeq H/l \approx 1$ per cent effective for a height $l \approx 10^3$ cm from the lower plate.

Since the gap height $G \approx 10^4$ cm, a hill of height 10 cm on the polar cap results in an average excess electric field of 0·1 per cent in the volume of the gap directly above it. We shall now show that even such a small excess electric field can significantly alter the number of charged particles produced in the gap.

Let us think of the spark discharge as developing in time 'steps' where the number of charges multiply by a constant factor at the end of each step. During the development of the discharge there is continuous leakage of charges from the gap as they reach one or other ' plate ' of the capacitor. If for some reason the number of charges effective for further multiplication in each step were increased, say by a fraction ϵ, then in each step, the number of charges participating in the avalanche breakdown would be $(1+\epsilon)$ times more; in m steps the fractional increase in the total number of charges produced would be $(1+\epsilon)^m$.

In the RS model the fraction of charges effective in the multiplication is determined by the gap height G and $\lambda = \lambda_e + \lambda_{ph}$ where λ_e is the mean free path for charges to radiate a photon of the appropriate energy and λ_{ph} the mean free path for this photon to produce a pair in the gap magnetic field. We now define the time step as $G/2c$, which is the mean time taken by particles presently in the gap to leave it and be replaced by the next generation. If the density of charges is assumed uniform in the gap it will be seen that the fraction that will contribute to the next generation is $\eta \approx (1-\lambda/G)$; if $\lambda > G$, avalanche growth cannot occur. Now the charged particles radiate all along their path (except for the first λ_e cm) on the curved magnetic field lines even as they are accelerated by the gap electric field. An excess electric field in the gap would give the charges a little more energy at each point on their path provided that their energy is not limited by radiation reaction. This would result in an increased gamma of the charges accelerated over hills, where $\gamma = E/mc^2$. For 0·1 per cent average excess field,

$$\frac{\Delta\gamma}{\gamma} \approx 1/1000.$$

But curvature photon energy (E_{ph}) is proportional to γ^3. Therefore

$$\frac{\Delta E_{ph}}{E_{ph}} \approx \frac{3\Delta\gamma}{\gamma} \approx \frac{3}{1000}.$$

This would reduce λ_{ph} which is given by $\lambda_{ph} \propto e^{4/3\chi}$, where χ is proportional to the energy of the photon, and is typically $\approx 1/15$ (Ruderman and Sutherland 1975). We thus have

$$\frac{\Delta\chi}{\chi} \approx \frac{3}{1000},$$

$$\text{or } -\frac{\Delta\lambda_{ph}}{\lambda_{ph}} \approx 0{\cdot}06.$$

If we assume

$$\lambda_e < \lambda_{ph}, \frac{\Delta\lambda}{\lambda} \approx \frac{\Delta\lambda_{ph}}{\lambda_{ph}}$$

and we can compare η in the two cases, which differ in the values of λ in the following form:

$$\epsilon = \Delta\eta/\eta = -\frac{\Delta\lambda}{G} \times \Theta \text{ where } \Theta = \frac{1}{\left(1 - \frac{\lambda}{G}\right)}.$$

If we assume $\lambda \approx 5 \times 10^3$ cm (Ruderman and Sutherland 1975) $\Theta \approx 2$ but could be much larger if λ were closer to G. Spark discharges over a hill therefore would contain $\left(1 + \frac{2\Delta\lambda}{G}\right)$ times more charges at the end of each 'step'. As the time for one spark discharge $\approx 10^{-5}$ s the number of 'steps' in which the avalanche growth is completed is $\frac{10^{-5} \times 2c}{G} \approx 60$. In 60 steps the fractional increase in the total number of charges in the gap is

$$\left(1 + 2\frac{\Delta\lambda_{ph}}{G}\right)^{60} = (1 + 0.06)^{60} \approx 30.$$

As the radio emission is produced by positrons subsequent to their entering the magnetosphere the average radio intensity could well be expected to depend on the number of particles. Further because of the coherent nature of the radio radiation it is not unreasonable to expect it to be proportional to some power (larger than 1) of the number of particles that are produced in each spark. At the present state of

understanding it is difficult, if not hopeless, to take into account all these considerations and to calculate the expected increase in average pulse intensity produced by sparks over hills. Our aim has been merely to show that such an increase is likely, critically dependent on the electric field in the gap, and easily capable of accounting for the observations which show a variation in intensities across the pulse window by factors of the order of $\approx 10^2$. It should be noted however that unless hills of height at least 5 cm (half the assumed value) can be supported on pulsar polar caps, the mechanism described above cannot satisfactorily account for the observations.

4. Deformation of the polar cap by sparks

In this section we will discuss the possible effect of sparks on the polar cap. In the vacuum gap both electrons and positrons are produced and are accelerated towards opposite ends of the gap. Since both types of charges are accelerated by the same electric field they gain similar energies. Therefore the electrons striking the polar cap surface must carry the same energy as the positrons which produce the observed radiation from the pulsar. As the typical total luminosity of a pulsar is $\geqslant 10^{30}$ erg s^{-1} we can expect the electrons in the spark to dump this order of energy onto the polar cap of the pulsar. Any damage done to the surface by these electrons will depend upon the structure and composition of the surface material and the details of the energy dissipation process.

We could begin by asking what are the various things that could happen to the surface as a result of a spark at a certain point on it. One possibility is what has been generally believed so far, *i.e.*, there will be local heating, consequently some excess radiation of photons and no change in the topography. At the other extreme it is conceivable that a pit is formed at the position of a spark and pieces of the crust are thrown up and scattered around the pit. A more likely possibility, however, is a very slight deformation of the crustal surface with the matter remaining bound at all stages; the energy required to create slips is very much less than the energy required to break the bonds between iron atoms.

If the energy available in each spark can effect some rearrangement of matter due to flow of material after sparking, we suggest that the result of a spark on the polar cap will be to *raise* the surface at that point by a minute amount. Although such a hypothesis might seem unlikely by analogy with the effect of meteorites and other energetic solid matter impinging on the surface of planets, we propose that it can happen in the case of pulsars. The very strong electric field at the surface of the polar cap is operative in the sense of trying to tear out ions from it against the force of gravity. The very basis of the RS model is the inability of this electric field to do so simply because of the high binding energy in the presence of strong magnetic fields. The positively charged outer crust at the magnetic polar cap may be likened to a pressurised balloon with a thin solid surface. A dimunition of the binding energy must therefore work in the sense of aiding a movement away from the centre of curvature of the crust. The duration of a spark can therefore be thought of as a short interval of time during which the cohesive energy of the lattice has been decreased, thus making it possible for the electric field to have its way and raise a tiny bump at the position of maximum heating.

The most favourable manner of raising bumps would involve stripping of atomic

electrons by the intense beam of spark electrons. This would *momentarily* leave the crust under the spark with a much higher positive charge. A variation of particle density across the spark would effect a similar variation in the extra surface charge density of the softened crustal material leading to a differential upward force. If, the spark were densest in the middle, as one would expect, then a small bump on the polar cap should be left behind by a spark. We saw in the previous section that surface variations on the polar cap of the order of 10 cm could lead to the intensity variations observed across integrated pulse profiles. If an individual spark can be effective in creating a minor deformation in the polar cap, then with time the amplitude of this deformation would increase even if sparking were completely random. An upper limit for Δh, the deformation required per spark, can be obtained from the observed correlation of complex pulse profiles with pulse periods in excess of 0·75 s. The typical age of a pulsar with a period of 0·75 seconds is $\geqslant 10^6$ years and this may be taken as the time for the surface relief of the polar cap to have build up to a root mean square value of $\sim$10 cm. Since there occurs one spark per millisecond on the average over any point on the polar cap, we have 3×10^{16} sparks corresponding to 10^6 years. On a purely random basis the peaks in the surface relief would have a height $\geqslant \sqrt{3\times 10^6}\times \Delta h \approx 10$ cm. This leads to a value of $\Delta h \approx 10^{-7}$ cm or the incredibly small value of 10 Å.

In other words, if a single spark managed to increase the height at its centre of impact by 10 Å, then over a period of the order of a million years the surface of the polar cap must end up with variations in height of the order of 10 cm and lead to the consequences discussed in the previous section. The amount of matter under a spark area that must be rearranged to obtain a bump of height 10 Å is $\sim 10^{26}$ atoms. The question is whether enough energy can be imparted to the surface layer in a way that will make it temporarily mobile and allow the electric tension to rearrange it.

Notions regarding the stability of the crustal material have been changing since the early work of Chen, Ruderman and Sutherland (1974) who derived a value for the cohesive energy for each iron atom of $\sim$10 keV. This number was revised by Flowers *et al.* (1977) according to whom the cohesive energy of iron per atom in a field of $\sim 10^{12}$ gauss is $\sim$2 keV. If a spark can impart at least this amount of energy to each of more than say 10^{26} atoms directly under the spark, there is then the possibility of rearrangement under the effect of the electric tension. The amount of energy carried by the electrons to the surface is 10^{30} erg s^{-1}. At the rate of 10^5 sparks per second, there is thus in each spark about 10^{25} erg. The area of the spark is $\pi\times 10^6$ cm^2. Assuming the generally accepted upper limit of 10^5 g cm^{-3} for the density at the surface, there is enough energy in the spark to give $\sim$2 keV per atom down to a depth of 1 cm. It is seen therefore, that if the energy is deposited in a much shorter distance, the atoms are bound to acquire much more than their cohesive energy immediately after each spark thus permitting a slight deformation within the radiation cooling time of the surface.

The heating of the surface under a spark has been discussed recently by Cheng and Ruderman (1980). According to them 'if a pair production discharge occurs above the polar cap an intensive flux of 10^{12} eV electrons is directed onto the surface causing strong local heating. This energy is deposited within $d \gtrsim 10$ radiation lengths (of the order of 10^{-3} cm in 10^5 g cm^{-3} of Fe) of the surface. It is largely re-radiated locally from the area under the discharge.' The temperature quoted by these authors for the surface is a quarter keV $\approx 2{\cdot}5\times 10^6$K. This implies a total radiation

loss of $\sim 10^{30}$ erg s^{-1} over the whole of the polar cap commensurate with our assumptions in the preceding paragraph.

If the energy in sparks is indeed *deposited* within 10^{-3} cm as suggested by Cheng and Ruderman (1980), then it appears to us that even allowing for the energy taken up by electrons and that radiated as photons, and errors in the various estimates, we must still have a much larger number of mobile atoms than we need. Under these circumstances an eventual modification of the polar cap relief seems inevitable.

It may be mentioned that *increase in height* of an area due to a spark on it represents a positive feed-back mechanism, since subsequent sparks over this area will carry more energy than sparks over neighbouring depressions. Although the extra energy may appear tiny, the effect is significant over the timescales required to build up a hill by a purely random process. As a result the minimum step required per spark will actually be less than the $\Delta h = 10$ Å which we estimated conservatively earlier. It may also be pointed out that for a similar reason it would be harder to build up surface relief if sparks created pits instead of bumps, in which case the feed-back would be negative.

We have seen how polar cap surface modification by sparks can lead to structure in the integrated pulse profile over the timescale in which pulsars acquire such profiles. By the same token it may be noted that the profiles will remain stable over such periods. From the number of spark areas within the polar cap we can arrive at the minimum scale length for surface irregularities as of the order of 10 metres. The maximum number of hills that one can expect to find along the diameter of a typical polar cap would therefore be ~ 10, and along a chord somewhat fewer. This is in good agreement with observations which show that the maximum number of major components in an integrated pulse profile is about 5. PSR 2045—16 has three major components and PSR 1237—25 has two major and three minor components. In the next section we shall discuss how similar structure in integrated profiles can result from minor magnetic field variations over the polar cap.

5. Magnetic field variations

In an earlier section we showed how the number of charges produced in a spark discharge depended critically on λ, the total path length within the gap for a charge to be accelerated, produce a photon, and for the photon to produce a pair. In that case, the variation in λ resulted mainly from the variation in λ_{ph}, the path length for a photon to produce a pair. It was also seen earlier that λ_{ph} depends critically on the energy of the photon, since $\lambda_{ph} \propto e^{4/3\chi}$, and χ is proportional to the photon energy. In this expression, χ is also proportional to the strength of the perpendicular component of the magnetic field. The angles made by the field lines within the gap with the trajectory of the gamma ray photons are very small, and the perpendicular component is therefore directly proportional to this small angle. Even a small change in this angle will therefore have a large effect on λ_{ph} with a consequent change in the total number of particles produced as discussed earlier. For example, an increase of 3 parts per thousand in the small angle made by the field lines with the photon trajectory will result in the same increase of a factor ≈ 30 in the total number of charges, as calculated earlier for a similar increase in the photon energy.

Given a pure dipole magnetic field the curvature of the field lines will vary smoothly

across the polar cap and will lead to pulse profiles that do not have a complicated or random structure. However, if pulsar fields evolve with time as discussed by Flowers and Ruderman (1977) multipole components will make their appearance in due course. Such multipole components even if present to a very small degree will significantly modify the curvature of the field lines in the polar cap. For the reasons discussed above this will then be strongly reflected in the intensity of the sparks produced at different longitudes *i.e.* structure in the integrated pulse profile.

To predict the effect of multipole components on the pulse structure is difficult because of the number of parameters involved in the addition of even a quadrupole component. Simple trial models seem to suggest that the major effect of the introduction of a quadrupole component in the gap field would be asymmetry in the pulse profile. The general result is to increase the curvature of the field lines on one side and to decrease it on the other. It seems much harder to create variations in the curvature of the field lines across the gap that could lead to a complex profile with many components as seen in several pulsars.

We note that if multipole fields in older pulsars are as inevitable and as strong as suggested by Flowers and Ruderman (1977), they must have a dominating influence on the pulse profile according to the conclusions drawn above. However, for the reasons just discussed the net result might be merely to make one part or region of the polar cap very much more effective than the rest. In such a case the observed profile would be interpreted as having a smaller duty cycle and might not be recognised as one modified by a complicated field structure in the gap. In any case we note that if multipole components can be shown to be responsible for variations in pulse structure, then this provides an observational method for determining the timescale for the evolution of the magnetic fields from the age of the pulsars which show such effects.

6. Discussion and conclusions

We have outlined two possible ways in which the complex variation of the mean intensity within pulse profiles could be explained. In one case, minute local deformations of the surface due to individual sparks lead to a build-up of a surface relief pattern on the polar cap; this in turn causes small variations in the electric field intensity within the gap leading to much larger variations of the number of positrons produced by the sparks. The second possibility invokes the presence of multipole components which modify the curvature of the magnetic field lines from point to point within the gap leading to the same conclusions as above.

Either mechanism provides general agreement with the observations in that the complicated pulse structure is correlated with older pulsars, and is stable for long periods. Also, the polarisation variation would be independent of the intensity structure within the pulse. In one case, the magnetic field structure would be unaffected by surface variations over the polar cap. For the other, multipole fields would need to modify the dipole pattern only marginally to account for the pulse intensity structure. Further, since they fall off much faster than the dipole field, their contribution in the radiating region at some distance from the pole will be greatly reduced. Hence for both mechanisms the sweep of the position angle of polarisation would be independent of the intensity variations across the pulse, as has been noted and emphasised by Manchester (1979).

To make an assessment from the observations of the importance of either of the two proposed mechanisms, one must take into account the pulse shapes obtainable in the absence of these or other such mechanisms. In magnetic pole models involving radiation into a hollow cone, both single and double pulse structures are easily explained in terms of edge and central cuts of the hollow cone by the line of sight. Many of the symmetry properties observed in pulses can be well accounted for by the circular symmetry of such a hollow cone. As pulses with complicated structure are generally from older pulsars, the radiating region would be further from the light cylinder than in younger (and faster) pulsars, and hence the asymmetry expected from sweeping back of the field lines would also be less. It is the presence of marked asymmetries and/or multiple components that cannot be accounted for in this way, and which we are attempting to explain in this paper.

We have seen earlier that a quadrupole component of the magnetic field can introduce a strong asymmetry, but is unlikely to create a complex pulse profile with many features. On the other hand, surface variations in the polar cap can produce both a large number of components and also asymmetry, since no particular symmetry will result from an essentially random process. Complex profiles, found (for example) in PSR 1237+25, seem therefore to strongly favour the polar cap relief hypothesis, whether or not the other mechanism also contributes. As mentioned earlier this is based on the assumption, which is hard to either prove or disprove at the moment, that the surface irregularities of the order of 10 cm can be supported on the polar cap. Further understanding of the structure and strength of neutron star crusts might show such an assumption to be untenable. If so, this would indicate that the alternative mechanism we have discussed is the operative one, and that the magnetic field structure of older pulsars can have at least some contributions of higher order than a quadrupole moment.

Acknowledgements

We thank Rajaram Nityananda and Ramesh Narayan for numerous discussions and help rendered during the course of this investigation. We are also grateful to D. Morris for a critical reading of the manuscript and to P.A.G. Scheuer for an elegant derivation relating to the maximum possible heights of hills.

References

Chen, H. H., Ruderman, M. A., Sutherland, P. G. 1974, *Astrophys. J.*, **191**, 473.
Cheng, A. F., Ruderman, M. A. 1977, *Astrophys. J.*, **214**, 598.
Cheng, A. F., Ruderman, M. A. 1980, *Astrophys. J.*, **235**, 576.
Cordes, J. M. 1976, *Astrophys. J.*, **208**, 944.
Ferguson, D. C., Graham, D. A., Jones, B. B., Seiradakis, J. H., Weilebinski, R. 1976, *Nature*, **260**, 25.
Flowers, E. G., Lee, J. F., Ruderman, M. A., Sutherland, P. G., Hillebrandt, W., Muller, E. 1977, *Astrophys. J.*, **215**, 291.
Flowers, E. G., Ruderman, M. A. 1977, *Astrophys. J.*, **215**, 302.
Hankins, T. H. 1971, *Astrophys. J.*, **169**, 487.
Irvine, J. M. 1978, *Neutron Stars*, Clarendon Press, Oxford.
Manchester, R. N. 1979, *New Zealand J. Sci.*, **22**, 479.
Ruderman, M. A., Sutherland, P. G. 1975, *Astrophys. J.*, **196**, 51.
Taylor, J. H., Huguenin, G. R. 1971, *Astrophys. J.*, **167**, 273.

THE ASTROPHYSICAL JOURNAL, 274:771–775, 1983 November 15

A NEW MODEL FOR THE EMISSION GEOMETRY IN PSR 0950+08

RAMESH NARAYAN AND M. VIVEKANAND
Raman Research Institute, Bangalore, India
Received 1982 September 9; accepted 1983 April 20

ABSTRACT

We propose that the angle between the magnetic and rotation axes in PSR 0950+08 is small, that the hollow radiation beam is highly elongated in the north-south direction (referred to the rotation axis) and extends beyond the rotation pole, and that the line of sight to Earth, which passes between the magnetic and rotation axes, intersects the same beam twice, on either side of the rotation pole, to produce the main and interpulse. The model fits the observed polarization angle variation well and explains most of the puzzling features noted in the interpulse. The geometry is distinctly different from that commonly invoked for double component pulsars.

Subject headings: pulsars — radiation mechanisms

I. INTRODUCTION

The radio pulsar PSR 0950+08 has an interpulse emission with many puzzling features which cannot be explained by current models. The bridge of emission between the main and interpulse (Hankins and Cordes 1981, hereafter HC) with a monotonic polarization angle variation (HC; Rankin and Benson 1981) rules out a two-pole model. However, the alternative hollow cone single-pole model of interpulses (Manchester and Lyne 1977) runs into difficulties over the marked asymmetry in many properties between the main and interpulse as well as the remarkable frequency independence of their separation (HC). HC have discussed the pros and cons of various possible models for this pulsar and argue that modified single-pole models, with nearly aligned magnetic and rotation axes, are the most promising candidates. We present here a single-pole model with certain novel features. The beam is much elongated along the meridian and straddles the rotation pole. Consequently, the line of sight intersects the same beam twice, at different offsets from the magnetic pole. Our model is in better agreement with polarization angle observations than other models. It also naturally explains the many apparently conflicting observations discussed above. If our model is correct, it gives new insight into the shape of pulsar beams, which could lead to a better understanding of pulsar physics.

II. THE MODEL

The model we present here for PSR 0950+08 is the result of our attempt to fit the excellent 430 MHz polarization angle variation observations of Backer and Rankin (1980). Their presentation of the data in the form of a histogram enables us to avoid complications from orthogonal radiation modes (Manchester, Taylor, and Huguenin 1975; Backer, Rankin, and Campbell 1976). Figure 1 shows the variation of the mean polarization angle θ with pulse longitude φ in one of the orthogonal modes in the main pulse and the interpulse.

We assume that the pulsar emission occurs above the magnetic poles of a rotating neutron star and that the polarization of the radio radiation reflects the orientation of the magnetic field at the point of emission (Radhakrishnan and Cooke 1969). We further assume that the magnetic field pattern is purely radial when projected on a plane perpendicular to the magnetic axis (as for a magnetic dipole). Backer and Rankin (1980) argue that there is strong evidence in their polarization data for the validity of these assumptions. We also assume that the pulsar emission at each frequency occurs at a constant height above the magnetic poles in a region well inside the light cylinder. This "radius-to-frequency" mapping of pulsar emission (Komesaroff 1970; Cordes 1978) simplifies the emission geometry by restricting it to two dimensions and also avoids complications from differential aberrations and time delays. However, a recent study by Björnsson (1982) highlights the fact that three-dimensional pulse emission geometries are also possible.

Let α be the angle between the magnetic and rotation axes and β the angle between the line of sight to Earth and the rotation axis. Also, let θ_0 be the position angle in the sky of the projected direction of the pulsar rotation axis and φ_0 the pulse longitude at which the line of sight comes closest to the magnetic pole. The variation of the polarization position angle θ with pulse longitude φ in the Radhakrishnan-Cooke model is then given by (Manchester and Taylor 1977, eq. [10–24]).

$$\tan(\theta - \theta_0) = \frac{\sin\alpha \sin(\varphi - \varphi_0)}{\cos\alpha \sin\beta - \sin\alpha \cos\beta \cos(\varphi - \varphi_0)} . \quad (1)$$

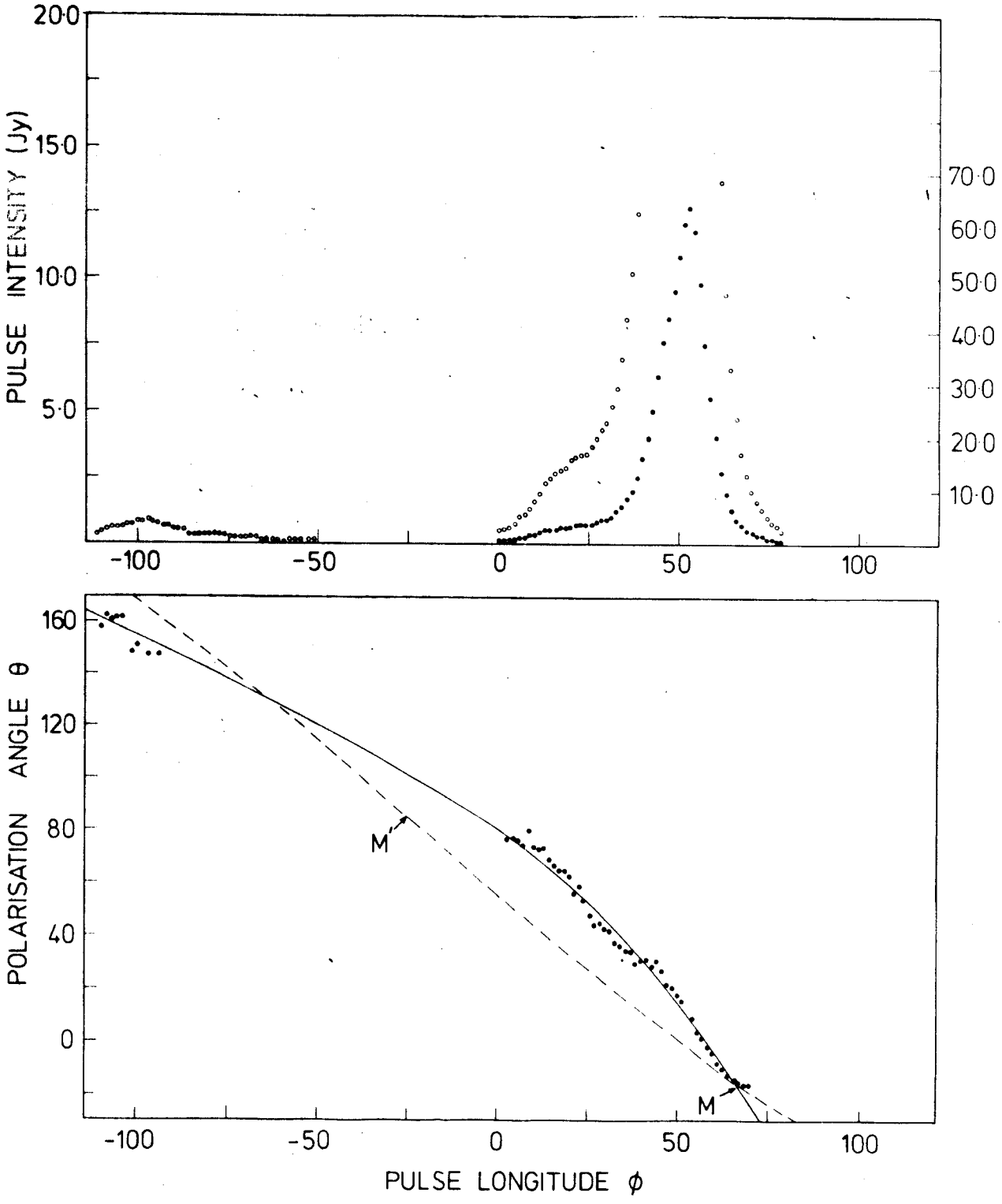

FIG. 1.—Least squares fit of the polarization angle variation across the main and interpulse of PSR 0950+08. The filled circles are mean polarization angles calculated from the detailed experimental results of Backer and Rankin (1980). The solid line is obtained with $\alpha = 10°$, $\beta = 5°$, M being the point of closest approach to the magnetic pole. The rms misfit in polarization angle is 3°8. The dashed line, which corresponds to the best fit hollow cone model with $\alpha = 30°$, $\beta = 5°$ and magnetic pole at M′, is seen to be a distinctly poorer fit. For comparison the integrated pulse profile is also shown.

We have made a least squares fit of the data in Figure 1 to a polarization angle variation of the above form by simultaneously optimizing the four unknown parameters α, β, φ_0, and θ_0. The solid line shows the fit corresponding to the best model, with $\alpha = 10°$, $\beta = 5°$. The point M represents the closest approach to the magnetic pole and corresponds to (φ_0, θ_0). We note two key features of this model: (*a*) Since both α and β are small, the line of sight is always close to one magnetic pole; it is therefore a single pole model with nearly aligned rotation and magnetic axes, as anticipated by HC. (*b*) The point M lies within the main pulse; hence the geometry, which is discussed in greater detail below, is quite different from the hollow cone model of interpulses (Manchester and Lyne 1977), where M should lie midway between the main and interpulse. We find that the least squares fit is very sensitive to the ratio β/α, fairly sensitive to the location of M (φ_0 could be moved a few degrees on either side provided θ_0 was also suitably adjusted) and quite insensitive to the value of α (which can lie between 0° and ~ 25°). The fit with the hollow cone model is found to be poor for all combinations of parameters tried. The dashed curve in Figure 1 shows one of the better hollow cone models with $\alpha = 30°$, $\beta = 5°$, and (φ_0, θ_0) corresponding to M′.

Figure 2 shows the geometry of the beam in our best fit model of PSR 0950+08 as viewed down the rotation axis. The main and interpulse are indicated by thick lines on the line-of-sight circle. A qualitative argument shows that this model is consistent with the polarization data. Narayan and Vivekanand (1982) have demonstrated that a monotonic polarization angle variation of the type shown in Figure 1 with no reversal in the sign of the slope implies that the line of sight must pass between the rotation and magnetic axes. Further, equation (1) shows that the derivative $|d\theta/d\varphi|$ attains its maximum value at the closest approach of the line of sight to the magnetic axis and vice versa. Although the polarization data of PSR 0950+08 shown in Figure 1 are unclear in this regard, the observations of Rankin and Benson (1981) for the same pulsar show rather unambiguously that $|d\theta/d\varphi|$ is larger in the main pulse than in the interpulse. Hence the locations of the main and interpulse on the line-of-sight circle are determined. In short, given our assumptions, the qualitative features of the geometry shown in Figure 2 are plausible even without having to do a least squares fit. We still have the freedom to draw the shape of the beam. To our mind, the most natural way to arrange the beam is to center it on the magnetic axis and elongate it in the "north-south" direction (north is defined with respect to the rotation axis) so that it extends well beyond the rotation pole and crosses the line of sight on the other side to make the interpulse. The dashed line in Figure 2 shows a possible beam outline. Since the outer extremities of the main and interpulse have been selected to have the same

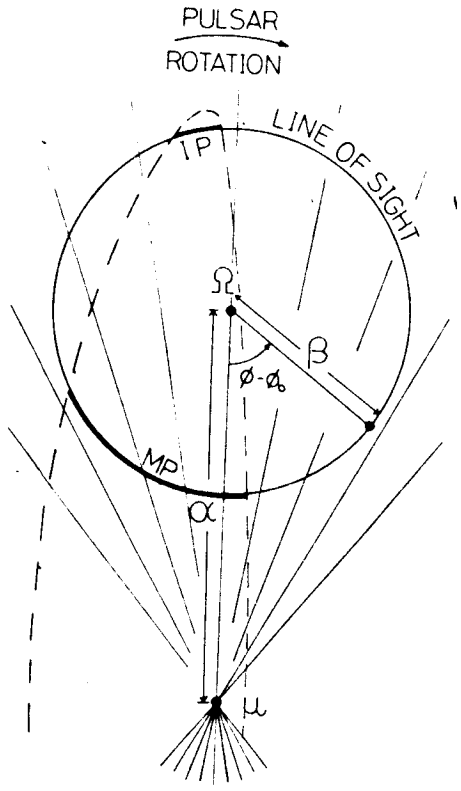

FIG. 2.—Proposed geometry of PSR 0950+08 projected down the rotation axis. The figure is to scale and shows the relative projected positions of the rotation axis Ω, the magnetic axis μ, the main pulse MP, and the interpulse IP, corresponding to the least squares fit of Fig. 1. The magnetic field lines are great circles but have been represented as radial straight lines. The dashed line is our suggestion for the shape (constant intensity contour) of the beam. Note the extreme elongation in the north-south direction.

intensity (~ 0.6 Jy at 430 MHz), this may be considered a constant power contour. We note that the north-south dimension of the beam is more than 5 times larger than the east-west dimension.

Apart from fitting the polarization observations, the above model explains many of the other puzzling features noted in PSR 0950+08. (*a*) The pronounced difference in intensity between the main and interpulse can be explained as arising because the main pulse is much closer to the magnetic pole. (There is some observational evidence, e.g., Narayan and Vivekanand 1982, 1983, that, apart from the hollow portion of the pulsar beam, the radio intensity falls off monotonically with increasing latitude offset between the line of sight and the magnetic pole.) Also, the splitting of the main pulse into two components at low frequencies (HC) can be explained by invoking an elliptic hollow conical beam with a frequency dependent size. The interpulse, being a peripheral cut of the beam, is not expected to bifurcate. (*b*) The main and interpulse half-power widths as well

as the separation of the main pulse components could have frequency dependence, for example due to radius to frequency mapping (Komesaroff 1970; Cordes 1978). However, the main-to-interpulse separation is expected to be frequency-independent in our model as it is a geometrical quantity (see Fig. 2). This is in accord with observations (HC). (*c*) The bridge of emission between the main and interpulse with a monotonic polarization angle variation (HC; Rankin and Benson 1981) is natural since, as Figure 2 shows, the line of sight is always close to the beam. The bridge is expected to be stronger between the main pulse and the previous interpulse than the postinterpulse (in conformity with the observations of HC). (*d*) The similarity of microstructure morphology (Hankins and Boriakoff 1981) and the correlation of pulse intensities between the main and interpulse (HC) are consistent with our single pole model. The fact that the intensity of the interpulse follows the main pulse and not vice versa might mean that changes take place first near the center of the beam and then propagate outward. (*e*) The anomalously large width of the main pulse (78°) is consistent with the polar line of sight (small values of α and β).

The model does not automatically explain the 155° spacing between the main and interpulse. The beam has to be displaced to one side of the magnetic pole as in Figure 2. This rather unnatural feature may be caused by obscuration of part of the beam on one side. It could also occur due to sweep back of the magnetic field lines as the pulsar rotates, though in this case the analysis becomes complicated since the location at which radiation is sampled no longer follows the circular line-of-sight curve of Figure 2. We note in this connection that if we relax the assumption of radius-to-frequency mapping, then the 155° spacing can be explained by a time delay due to the interpulse radiation being emitted from closer to the neutron star. The altitude differential needed is $0.44 r_L$, where r_L is the light cylinder radius. This is only a small fraction of the distance from the neutron star surface to the light cylinder along the line-of-sight direction, which is $11.5 r_L$ for $\beta = 5°$.

III. DISCUSSION

The least squares fit we have made of the polarization angle variation in PSR 0950+08 is based on the Radhakrishnan-Cooke model coupled with radius-to-frequency mapping. Although the evidence so far seems to be in favor of this picture, this limitation should be kept in mind. If some of our assumptions are relaxed, the variation of polarization angle with pulse longitude may cease to be of the form (1), and it is not clear how the results will change. The case for a nearly aligned rotator model is probably still strong, but the shape and location of the beam in Figure 2 may possibly change. However, we note that our model does not rely solely on the polarization observations. Since it explains most of the other puzzling observations as well, we feel it must be correct in many of its details. If so, there are some important implications for our understanding of pulsars in general.

The most striking feature of the model is the large elongation of the beam. By means of least squares fits on other polarization angle observations, Narayan and Vivekanand (1982) estimated large values for the latitude offset $|\alpha - \beta|$ in several pulsars. This might imply that elongated beams are the rule rather than the exception. There is further support for this in a statistical study of the total polarization angle swing in pulsars (Narayan and Vivekanand 1983; see also Jones 1980). However, current theories of pulsar electrodynamics (based on the polar cap model) conventionally assume circular or near-circular beams. It is not clear how these theories can be reconciled with the large elongation we propose in PSR 0950+08 (it should be noted that the elongation ratio, which is > 5 in our model, is determined essentially by β/α and is very tightly constrained by the least squares fit). In many pulsar theories, the beam dimensions are determined by the last "closed" magnetic-field lines (Goldreich and Julian 1969). For pulsars with aligned magnetic and rotation axes (our model is a nearly aligned case), the beam cross section should be circular while for "orthogonal" pulsars it should be elongated (in the *east-west direction*!). Non-dipole magnetic field configurations might possibly explain the beam shape. Barnard and Arons (1982) included quadrupole field configurations and found that pulsar beams are elliptical in general. However, since the beams seem to be always elongated in the north-south direction (Jones 1980; Narayan and Vivekanand 1982, 1983), this would require a preferred orientation for the quadrupole axis with respect to the rotation and dipole axes, and it is not clear why it should be so.

The beam in our model extends on either side of the rotation pole and intersects the line of sight at nearly diametrically opposite regions. This unusual geometry would be rather unnatural in the light cylinder model of pulsar emission (e.g., Smith 1977).

For the first time we have a pulsar where the line of sight intersects the same beam at two different distances from the magnetic pole. We find further confirmation that the radio intensity falls away with increasing line of sight offset from the magnetic pole along the meridian and that nearer cuts give double component pulses while farther cuts give only a single component.

We gratefully thank R. Nityananda for help with spherical trigonometry and V. Radhakrishnan for several useful discussions. We also thank the referee for several illuminating comments on radius to frequency mapping and for suggesting that the 155° separation between the main pulse and interpulse could be explained by a time delay.

REFERENCES

Backer, D. C., and Rankin, J. M. 1980, *Ap. J.*, **42**, 143.
Backer, D. C., Rankin, J. M., and Campbell, D. B. 1976, *Nature*, **263**, 202.
Barnard, J. J., and Arons, J. 1982, *Ap. J.*, **254**, 713.
Björnsson, C.-I. 1982, ESO Scientific Preprint, 225.
Cordes, J. M. 1978, *Ap. J.*, **222**, 1006.
Goldreich, P., and Julian, W. M. 1969, *Ap. J.*, **157**, 869.
Hankins, T. H., and Boriakoff, V. 1981, *Ap. J.*, **249**, 238.
Hankins, T. H., and Cordes, J. M. 1981, *Ap. J.*, **249**, 241 (HC).
Jones, P. B. 1980, *Ap. J.*, **236**, 661.
Komesaroff, M. M. 1970, *Nature*, **225**, 612.
Manchester, R. N., and Lyne, A. G. 1977, *M.N.R.A.S.*, **181**, 761.
Manchester, R. N., and Taylor, J. H. 1977, *Pulsars* (San Francisco: Freeman).
Manchester, R. N., Taylor, J. H., and Huguenin, G. R. 1975, *Ap. J.*, **196**, 83.
Narayan, R., and Vivekanand, M. 1982, *Astr. Ap.*, **113**, L3.
———. 1983, *Astr. Ap.*, **122**, 45.
Radhakrishnan, V., and Cooke, D. J. 1969, *Ap. Letters*, **3**, 225.
Rankin, J. M., and Benson, J. M. 1981, *A.J.*, **86**, 418.
Smith, F. G. 1977, *Pulsars* (Cambridge: Cambridge University Press).

RAMESH NARAYAN and M. VIVEKANAND: Raman Research Institute, Bangalore-560 080, India

APPENDIX A

Let the sale height of electrons be z_0

$$\text{i.e.,} \quad n_e(z) = n_e(0)\, \text{ExP}-(|z|/z_0) \tag{A.1}$$

Consider a pulsar at height z and galactic latitude b_{II} (hence distance $d = |z| / \sin b_{II}$). Its dispersion measure is given by

$$DM = \frac{n_e(0)\, z_0}{|\sin b_{II}|} \left[1 - \text{ExP}-(|z|/z_0) \right] \tag{A.2}$$

The mean elecctron density for this pulsar is

$$\langle n_e(z) \rangle = \frac{n_e(0)\, z_0}{|z|} \left[1 - \text{ExP}-(|z|/z_0) \right] \tag{A.3}$$

Let pulsars also be distributed exponentially with scale height z_p. Then the effective electron density for the whole pulsar population is

$$\langle n_e \rangle = \frac{n_e(0)\, z_0}{z_p} \int_0^\infty \frac{1}{z} \left[1 - \text{ExP}-(z/z_0) \right] \text{ExP}-(z/z_p)\, dz \tag{A.4}$$

$$= \frac{n_e(0)\, z_0}{z_p} \ln \left[1 + z_0/z_p \right]$$

Taking z_0 =70 pc (as for HII regions) and z_p =350 pc, we obtain

$$\langle n_e \rangle = 0.358\, n_e(0) \tag{A.5}$$

APPENDIX B

If an HII region lies along the line of sight to a pulsar, it contributes to the dispersion measure (DM). Since pulsar distances are derived using DM , the HII region contribution must be subtracted. Prentice and ter Haar (1969) have given a scheme for estimating the corrections. However, their results might be inaccurate because of unknown parameters, such as Strömgren radii and electron densities of the HII regions. The inaccuracies could be particularly serious if the HII region contribution is a major fraction of the pulsar's DM . Therefore we have "softened" the Prentice-ter Haar correction using the following scheme.

We postulate that the dispersion measure correction of an HII region has a rectangular probability distribution as shown in fig. B.1 where H is the correction given by Prentice and ter Haar. We average the calculated distance to the pulsar over this probability distribution and use averaged distances in our studies. Let d be the DM left to be accounted for just at the front face of the HII regions. It is easy to see that whenever $d \gg 3H/2$ or $d \leq H/2$, the present scheme gives practically the same distances as the old scheme (which directly used the single value of H). For the case

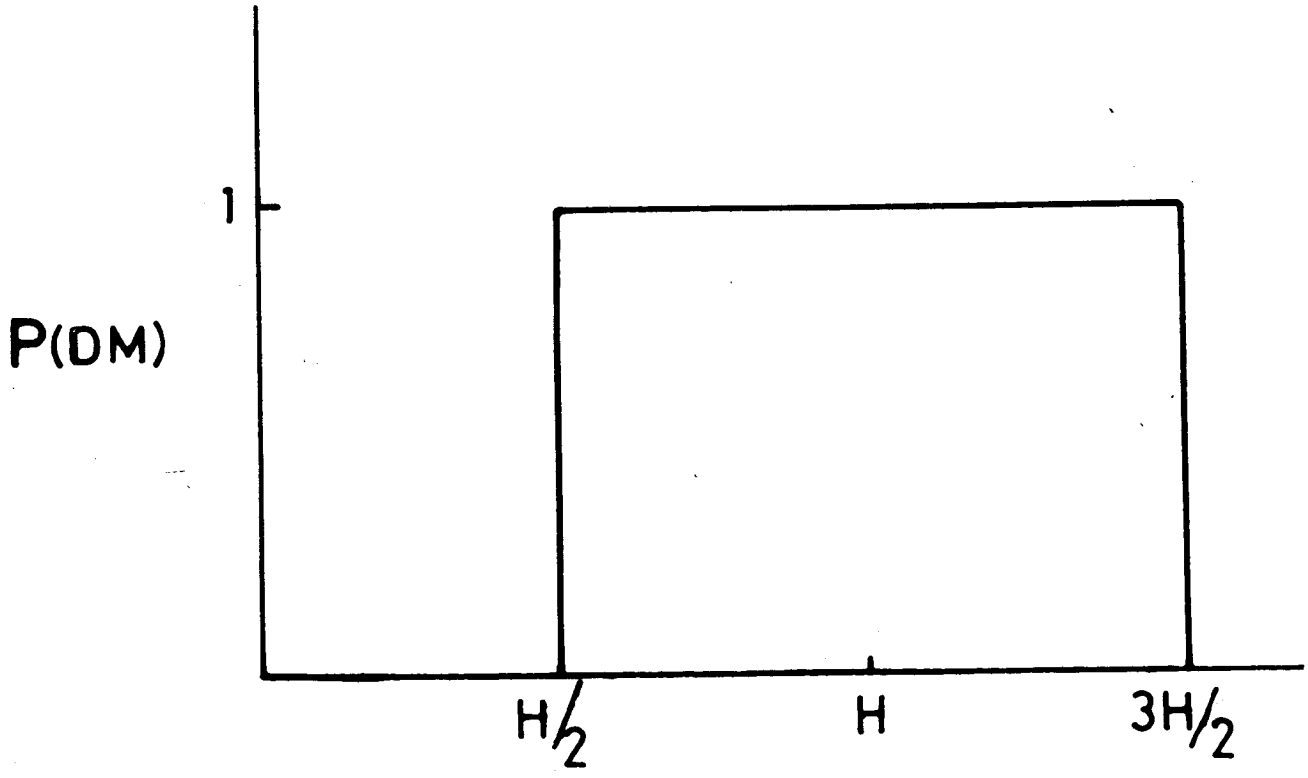

FIG. B.1 : Assumed probability distribution of the dispersion measure correction (H) due to HII regions.

$H/2 < d < 3H/2$, the new scheme gives a larger estimate for the pulsar distance than the old. A larger distance implies a larger estimate for the pulsar luminosity L and hance a smaller estimate for the scale factors $S(L, P)$. We are thus, in a sense, being conservative and erring on the side of slightly underestimating the quantities of interest.

APPENDIX C

In various sections of chapter 4, we are interested in evaluating quantities of the form

$$Q = \int x\, p(x)\, dx \tag{C.1}$$

where x is some property of pulsars and $p(x)\,dx$ is the probability of observing a pulsar having a value of this property in the range x to $x + dx$. We estimate Q by means of the following sum over the x_i of the observed pulsars

$$Q_{est} = \sum_{i=1}^{N} x_i \tag{C.2}$$

Now the probabilities of observing pulsars in different ranges of x are independent of one another. Hence, Q in eq. (C.1) is the weighted integral over independent poisson variables (of mean $p(x)\,d(x)$). The variance of Q is then clearly given by

$$V = \int x^2 p(x)\, dx \tag{C.3}$$

This can be estimated in terms of the observed pulsars by means of

$$V_{est} = \sum_{i=1}^{N} x_i^2 \tag{C.4}$$

which is the formula used throughout chapter 4.

The form of V in eq. (C.3) is different from the following more usual form .

$$V' = \int (x - \bar{x})^2 p(x)\, dx$$

$$= \int x^2 p(x)\, dx - \bar{x}^2 \int p(x)\, dx \qquad (C.5)$$

The difference arises because the variance in the present case (eq. (C.3)) has two contributions:

(a) There is one contribution arising from the distribution of values of x , giving an expression exactly of the form eq. (C.5).

(b) Secondly, being a poisson process, the total number of observed pulsars

$$N = \int p(x)\, dx \qquad (C.6)$$

can itself fluctuate, i.e., there can be fluctuations in the number of terms in eq. (C.2). It is easily verified that this contribution cancels the second term in eq. (C.5), leading to eq. (C.3).

APPENDIX D

As already mentioned in chapter 4, we expect the distribution of θ_{est} (eq. C.2) to be asymmetric, with a long tail, because only a few top values of X_i usually contribute to the result. Therefore we prefer to use confidene limits rather than the standard deviation. In computing the confidence limits, We assume that our estimate $\theta_{est} = \sum_{i=1}^{N} X_i$ is the sum of N random Poisson variables (v_i) of mean equal to 1, each weighted by the respective X_i .

$$\theta_{est} = \sum_{i=1}^{N} v_i X_i \qquad (D.1)$$

By numerically generating N random variables between 0 and 1, we generate N random Poisson variables with mean 1 and therefore a random value of θ_{est} . By generating many random values of θ_{est} , we then estimate the probability distribution of θ . The confidence limits are then easily marked off by measuring areas under this probability curve.

REFERENCES

(1) Ables J. G. and Manchester R. N., 1976, ASTRON. ASTROPHYS., 50, 177.

(2) Anderson B., Lyne A. G. and Peckham R. J., 1975, NATURE, 258, 215.

(3) Arnaud M. and Rothenflug R., 1980, ASTRON. ASTROPHYS., 87, 196.

(4) Arnett W. D. and Lerche I., 1981, ASTRON. ASTROPHYS., 95, 308.

(5) Arons J., 1979, SPACE SCI. REV., 24, 437.

(6) Baade W. and Zwicky F., 1934, PROC. NAT. ACAD. SCI., 20, 254.

(7) Backer D. C. and Rankin J.M., 1980, ASROPHYS. J. SUPPL. SER., 42, 143.

(8) Backer D. C., Rankin J. M. and Campbell D. B., 1976, NATURE, 263, 202.

(9) Backer D. C. and Sramek R. A., 1976, ASTRON. J., 81, 1430.

(10) Bartel N., Morris D., Sieber W. and Hankins T. H., 1982, ASTROPHYS. J., 258, 776.

(11) Baym G. and Pethick C., 1975, ANN. REV. NUCLEAR. SCI., 25, 27.

(12) Chanmugam G., 1973, ASTROPHYS. J. (LETTERS), 182 L39.

(13) Chen H. H., Ruderman M. A. and Sutherland P. G., 1974, ASTROPHYS. J. 191, 473.

(14) Cheng A. F. and Ruderman M. A., 1980, ASTROPHYS. J., 235, 576.

(15) Clark D. H. and Caswell J. L., 1976, MON. NOT. ROY. ASTRON. SOC., 174, 267.

(16) Clark D. H. and Stephenson F. R., 1977, MON. NOT. ROY. ASTRON. SOC., 179, 87p.

(17) Cole T. W., 1969, NATURE, 221, 29.

(18) Craft H. D., Comella J. M. and Drake F. D., 1968, NATURE, 218, 1122.

(19) Crovisier J., 1978, ASTRON. ASTROPHYS., 70, 43.

(20) Davies J. G., Horton P. W., Lyne A. G., Ricket B. J. and Smith F. G., 1968, NATURE, 217, 910.

(21) Davies J. G., Hunt G. C. and Smith F. G., 1969, NATURE, 221, 27.

(22) Davies J. G., Lyne A. G. and Seiradakis J. H., 1972, NATURE, 240, 229. (JODRELL BANK SURVEY)

(23) Davies J. G., Lyne A. G. and Seiradakis J. H., 1973, NATURE PHY. SCI., 244, 84. (JODRELL BANK SURVEY)

(24) Davies J. G., Lyne A. G. and Seiradakis J. H., 1977, MON. NOT. ROY. ASTRON. SOC., 179, 635.

(25) Davis L. and Goldstein M., 1970, ASTROPHYS. J. (LETTERS), 159, L81.

(26) de Loore C., de Greve J. P. and de Cuyper J. P., 1975, ASTROPHYS. SPACE. SCI., 36, 219.

(27) del Romero A. and Gomez-Gonzalez J., 1981, ASTRON. ASTROPHYS., 104, 83.

(28) Downes D., 1971, ASTRON. J., 76, 305.

(29) Ewart G. M., Guyer R. A. and Greenstein G., 1975, ASTROPHYS. J., 202, 238.

(30) Ferguson D. C., 1983, COMMENTS ON ASTROPHYSICS, 9, 127.

(31) Flowers E. G. and Ruderman M. A., 1977, ASROPHYS. J., 215, 302.

(32) Flowers E. G., Lee J. F., Ruderman M. A., Sutherland P. G., Hillebrandt W. and Muller E., 1977, ASTROPHYS. J., 215, 291.

(33) Gailly J. L., Lequeux J. and Masnou J. L., 1978, ASTRON. ASTROPHYS., 70, L15.

(34) Gold T. 1968, NATURE, 218, 731.

(35) Goldreich P., 1970, ASTROPHYS. J. (LETTERS), 160, L11.

(36) Goldreich P. and Julian W. H., 1969, ASTROPHYS. J., 157, 869.

(37) Groth E. J., 1975, ASTROPHYS. J. SUPPL. SER., 29, 453.

(38) Guseinov O. H. and Kasumov F. K., 1979, ASTROPHYS. SPACE SCI., 59, 285.

(39) Hall A. N., 1980, MON. NOT. ROY. ASTRON. SOC., 191, 751.

(40) Hankins T. H., 1981, in PULSARS, I. A. U. Symposium No. 95, D. Riedel Publishing Co., Dordrecht; eds W. Sieber and R. Wielebinski.

(41) Hankins T. H. and Cordes J. M., 1981, in PULSARS, I. A. U. Symposium No. 95, D. Riedel Publishing Co.,

Dordrecht; eds W. Sieber and R. Wielebinski.

(42) Harding D. S. and Harding A. K., 1982, ASTROPHYS. J., 257, 603.

(43) Hewish A., Bell S. J., Pilkington J. D. H., Scott P. F. and Collins R. A., 1968, NATURE, 217, 709.

(44) Huguenin G. R., 1976, in METHODS OF EXPERIMENTAL PHYSICS, 12, part C, Academic Press, New York; ed M. L. Meeks.

(45) Hulse R. A. and Taylor J. H., 1974, ASTROPHYS. J., (LETTERS), 191, L59. (ARECIBO SURVEY)

(46) Hulse R. A. and Taylor J. H., 1975, ASTROPHYS. J. (LETTERS), 201, L55. (ARECIBO SURVEY)

(47) Illovaisky S. A. and Lequeux J., 1972, ASTRON. ASTROPHYS., 20, 347.

(48) Jones P. B., 1976, NATURE, 262, 120.

(49) Jones P. B., 1980, ASTROPHYS. J., 236, 661.

(50) Katgert P. and Oort J. H., 1967, B. A. N., 19, 239.

(51) Komesaroff M. M., 1970, NATURE, 225, 612.

(52) Krishnamohan S., 1981, MON. NOT. ROY. ASTRON. SOC., 197, 497.

(53) Kristian J., Visvanathan N., Westphal J. A. and Snellen G. H., 1970, ASTROPHYS. J., 162, 475.

(54) Kundt W., 1977, NATURWISSENSCHAFTEN, 64, 493.

(55) Kundt W., 1981, NATURE, 292, 865.

(56) Kundt W., 1982, private communication.

(57) Large M. I., 1971, THE CRAB NEBULA, I. A. U. Symposium No. 46, D. Reidel Publishing Co., Dordrecht, pp165.

(58) Large M. I. and Vaughan A. E., 1971, MON. NOT. ROY. ASTRON. SOC., 151, 277.

(59) Large M. I., Vaughan A. E. and Mills B. Y., 1968, NATURE, 220, 340.

(60) Lyne A. G., 1981a, in PULSARS, I. A. U., Symposium No. 95, D. Reidel Publishing Co., Dordrecht; eds. W. seiber and R. Wielebinski.

(61) Lyne A. G., 1981b, in SUPERNOVAE: A SURVEY OF CURRENT RESEARCH, Proceedings of the NATO Advanced Study Institute, held at Cambridge, U. K.

(62) Lyne A. G., Anderson B. and Salter M. J., 1982, MON. NOT. ROY. ASTRON. SOC., 201, 503.

(63) Lyne A. G. and Ricket B. J., 1968, NATURE, 218, 326.

(64) Lyne A. G., Ritchings R. T. and Smith F. G., 1975, MON. NOT. ROY. ASTRON. SOC., 171, 579.

(65) Lyne A. G. and Smith F. G., 1968, NATURE, 218, 124.

(66) Manchester R. N., 1971, ASTROPHYS. J. SUPPL., 23, 283.

(67) Manchester R. N., 1979, AUSTR. J. PHYS., 32, 1.

(68) Manchester R. N., Lyne A. G., Taylor J. H., Durdin J. M., Large M. I. and Little A. G., 1978, MON. NOT. ROY. ASTRON. SOC., 185, 409. (IIMS)

(69) Manchester R. N. and Taylor J. H., 1977, PULSARS, W. H. Freeman and Co., San Fransisco.

(70) Manchester R. N. and Taylor J. H., 1981, ASTRON. J., 86, 1953.

(71) Mancheser R. N., Taylor J. H. and Huguenin G. R., 1975, ASTROPHYS. J., 196, 83.

(72) Manchester R. N., Taylor J. H. and Van Y. Y., 1974, ASTROPHYS. J. (LETTERS), 189, L119.

(73) McCulloch P. M., Hamilton P. A., Ables J. G. and Komesaroff M. M., 1976, MON. NOT. ROY. ASTRON. SOC., 175, 71p.

(74) McCulloch P. M., Hamilton P. A., Manchester R. N. and Ables J. G., 1978, MON. NOT. ROY. ASTRON. SOC., 183, 645.

(75) McKee C. F. and Ostriker J. P., 1977, ASTROPHYS. J., 218, 148.

(76) Melrose D. B., 1981, in PULSARS, I. A. U. Symposium No. 95, D. Reidel Publishing Co., Dordrecht; eds. W. Seiber and R. Weilebinski.

(77) Michel F. C., 1982, REV. MODERN PHYSICS, 54, 1.

(78) Michel F. C. and Goldwire H. C., 1970, ASTROPHYS. LETTERS, 5, 21.

(79) Minkowski R., 1942, ASTROPHYS. J., 96, 199.

(80) Milne D. K., 1970, AUSTR. J. PHYS., 23, 425.

(81) Narayan R. and Vivekanand M., 1981, NATURE, 290, 571.

(82) Narayan R. and Vivekanand M., 1982, ASTRON. ASTROPHYS., 113, L3.

(83) Narayan R. and Vivekanand M., 1983, ASTROPHYS. J., 274, 771.

(84) Newton L. M., Manchester R. N. and Cooke D. J., 1981,

MON. NOT. ROY. ASTRON. SOC., 194, 841.

(85) Oort J. H., 1977, ANN. REV. ASTRON. ASTROPHYS., 15, 295.

(86) Ostriker J. P., 1968, NATURE, 217, 1127.

(87) Ostriker J. P. and Gunn J. E., 1969, ASTROPHYS. J., 157, 1395.

(88) Pacini F., 1967, NATURE, 216, 567.

(89) Pacini F., 1968, NATURE, 219, 567.

(90) Pacini F. and Salpeter E. E., 1968, NATURE, 218, 733.

(91) Phinney E. S. and Balndford R. D., 1981, MON. NOT. ROY. ASTRON. SOC., 194, 137.

(92) Poveda A. and Woltjer L., 1968, ASTRON. J., 73, 65.

(93) Preintce A. J. R. and ter Haar D., 1969, MON. NOT. ROY. ASTRON. SOC., 146, 423.

(94) Radhakrishnan V., 1981, Preprint.

(95) Radhakrishnan V. and Cooke D. J., 1969, ASTROPHYS. LETTERS, 3, 225.

(96) Radhakrishnan V., Cooke D. J., Komesaroff M. M. and Morris D., 1969, NATURE, 221, 443.

(97) Radhakrishnan V., Komesaroff M. M. and Cooke D. J., 1968, NATURE, 218, 229.

(98) Rankin J. M. and Benson J. M., 1981, ASTRON. J., 86, 418.

(99) Richards D. W. and Comella J. M., 1969, NATURE, 222, 551.

(100) Robinson B. J., Cooper B. F. C., Gardiner F. F., Wielebinski R. and Landecker T. L., 1968, NATURE, 218, 1143.

(101) Ruderman M. A., 1972, ANN. REV. ASTRON. ASTROPHYS., 10, 427.

(102) Ruderman M. A. and Sutherland P. G., 1975, ASTROPHYS. J., 196, 51.

(103) SHKLOVSKI I. S., 1982, SOV.ASTRON. LETTERS, 8, 188.

(104) Skilling J., 1968, NATURE, 218, 923.

(105) Smith F. G., 1970, MON. NOT. ROY. ASTRON. SOC., 149, 1.

(106) Smith F. G., 1973, NATURE, 243, 207.

(107) Srinivasan G. and Dwarakanath K. S., 1982, J. ASTROPHYS. ASTR., 3, 351.

(108) Staelin D. H. and Reifenstein E. C., 1968, SCIENCE, 162, 1481.

(109) Sturrock P. A., 1971, ASTROPHYS. J., 164, 529.

(110) Tammann G. A., 1974, in SUPERNOVAE AND SUPERNOVA REMNANTS, D. Reidel Publishing Co., Dordrecht; ed C. B. Cosmovici.

(111) Tammann G. A., 1977, ANN. N. Y. ACAD. SCI., 302, 61.

(112) Taylor J. H., 1981, in PULSARS, I. A. U. symposium No. 95, D. Riedel Publishing Co., Dordrecht; eds W. Sieber and R. Wielebinski.

(113) Taylor J. H. and Huguenin G. R., 1971, ASTROPHYS. J., 167, 273.

(114) Taylor J. H. and Manchester R. N., 1977, ASTROPHYS. J., 215, 885.

(115) Trimble V., 1982, REV. MODERN. PHYSICS., 54, 1183.

(116) Vivekanand M. and Narayan R., 1981, J. ASTROPHYS. ASTR., 2, 315. (VN)

(117) Vivekanand M. and Narayan R., 1982, J. ASTROPHYS. ASTR., 3. 399.

(118) Vivekanand M., Narayan R. and Radhakrishnan V., 1982, J. ASTROPHYS. ASTR., 3, 237.

(119) Vivekanand M. and Radhakrishnan V., 1980, J. ASTROPHYS. ASTR., 1, 119.

(120) Zheleznyakov V. V., 1971, ASTROPHYS. SPACE. SCI., 13. 87.

(121) Zwicky F., 1962, in PROBLEMS OF EXTRAGALACTIC RESEARCH, I. A. U. Symposium No. 15, Macmillan Publishing Co. New York; ed G. C. Mcvittie.